

The Yeast Par-1 Homologs Kin1 and Kin2 Show Genetic and Physical Interactions with Components of the Exocytic Machinery

Maya Elbert,^{*†} Guendalina Rossi,^{†‡} and Patrick Brennwald^{‡§}

[‡]Department of Cell and Developmental Biology, University of North Carolina at Chapel Hill, Chapel Hill, NC 27599; and ^{*}Graduate Program in Pharmacology, Weill Medical College of Cornell University, New York, NY 10021

Submitted July 4, 2004; Revised October 28, 2004; Accepted November 11, 2004
Monitoring Editor: Keith Mostov

Kin1 and Kin2 are *Saccharomyces cerevisiae* counterparts of Par-1, the *Caenorhabditis elegans* kinase essential for the establishment of polarity in the one cell embryo. Here, we present evidence for a novel link between Kin1, Kin2, and the secretory machinery of the budding yeast. We isolated *KIN1* and *KIN2* as suppressors of a mutant form of Rho3, a Rho-GTPase acting in polarized trafficking. Genetic analysis suggests that *KIN1* and *KIN2* act downstream of the Rab-GTPase Sec4, its exchange factor Sec2, and several components of the vesicle tethering complex, the Exocyst. We show that Kin1 and Kin2 physically interact with the t-SNARE Sec9 and the Lgl homologue Sro7, proteins acting at the final stage of exocytosis. Structural analysis of Kin2 reveals that its catalytic activity is essential for its function in the secretory pathway and implicates the conserved 42-amino acid tail at the carboxy terminal of the kinase in autoinhibition. Finally, we find that Kin1 and Kin2 induce phosphorylation of t-SNARE Sec9 in vivo and stimulate its release from the plasma membrane. In summary, we report the finding that yeast Par-1 counterparts are associated with and regulate the function of the exocytic apparatus via phosphorylation of Sec9.

INTRODUCTION

Par-1 has been implicated in providing intracellular polarization cues in various biological systems. Initially, Par-1 has been described in *Caenorhabditis elegans* as one of the “partitioning” genes essential for anterior-posterior axis specification and asymmetry of zygote division (Kemphues *et al.*, 1988). Homologous genes have been characterized in *Schizosaccharomyces pombe* (*kin1+*) (Levin and Bishop, 1990), *Drosophila melanogaster* (*dPAR-1*) (Tomancak *et al.*, 2000), and mammalian cells (*mPARs*: p78, EMK, MARK) (Drewes *et al.*, 1995; Bohm *et al.*, 1997). The mechanism of cell polarity regulation by Par-1 seems to differ depending on the organism and the cellular context. Some reports link Par-1 function to restricting localization of polarity determinants: P granules and PIE-1 in *C. elegans* (Kemphues *et al.*, 1988; Tenenhaus *et al.*, 1998); Oscar, Orb, BicD, and Egl in *Drosophila* oocyte (Tomancak *et al.*, 2000; Huynh *et al.*, 2001; Vaccari and Ephrussi, 2002); and Par-3 via 14-3-3 in *Drosophila* follicular epithelium (Benton and Johnston, 2003). Others find that Par-1 regulates stability, density, and/or organization of the microtubule cytoskeleton as in *Drosophila* and mammalian cells (Drewes *et al.*, 1997; Shulman *et al.*, 2000; Cox *et al.*, 2001; Huynh *et al.*, 2001; Doerflinger *et al.*, 2003; Cohen *et al.*, 2004).

In the budding yeast *Saccharomyces cerevisiae*, the Par-1 counterparts Kin1 and Kin2 have been isolated by homology to the kinase family of viral oncogenes (Levin *et al.*, 1987). They belong to the Snf1 kinase family of the Ca²⁺/calmodulin-dependent kinase II (CaMK) group (Hanks *et al.*, 1988). Kin1 and Kin2 are structurally similar serine/threonine kinases with an N-terminally located catalytic domain and C-terminal regulatory domain (Lamb *et al.*, 1991; Donovan *et al.*, 1994). The catalytic core and the C-terminal 42-amino acid tail are highly conserved between *S. pombe*, *S. cerevisiae*, *C. elegans*, *D. melanogaster*, and mammalian orthologues of Par-1. Therefore, *S. cerevisiae*, as a polarized organism highly amenable to genetic analysis, represents an advantageous model to study yeast Par-1 orthologues. However, little is known about the function of Kin1 and Kin2 in *S. cerevisiae*.

This work investigates the role of Kin1 and Kin2 proteins in polarized exocytosis in yeast. In *S. cerevisiae*, polarity is manifested by asymmetric growth of the bud, which requires polarized transport of Golgi-derived vesicles and their subsequent docking and fusion with the plasma membrane at the bud tip. Golgi-to-plasma membrane transport is dependent on the actin cytoskeleton and Rho/Rab GTPases, such as Rho3, Cdc42, and Sec4. Definition of the docking site and vesicle tethering is mediated by a multiprotein Exocyst complex, comprised of eight subunits: Sec3, Sec5, Sec6, Sec8, Sec10, Sec15, Exo70, and Exo84 (Guo *et al.*, 1999). After docking, vesicle fusion with the plasma membrane involves correct pairing of one vesicle SNARE, Snc1/2, with two membrane t-SNAREs: Sso1/2 and Sec9 (Aalto *et al.*, 1993; Protopopov *et al.*, 1993; Brennwald *et al.*, 1994). Although the aforementioned molecules constitute the core of the secretory machinery, polarized exocytosis is fine-tuned by many additional components.

Article published online ahead of print in *MBC in Press* on December 1, 2004 (<http://www.molbiolcell.org/cgi/doi/10.1091/mbc.E04-07-0549>).

[†] These authors contributed equally to this work.

[§] Corresponding author. E-mail address: pjbrennw@med.unc.edu.

Here, we report that yeast Par-1 orthologues regulate exocytosis. We show that Kin1 and Kin2 genetically interact with multiple components of the late exocytic machinery and physically associate with the t-SNARE Sec9 and the SNARE-binding protein Sro7. We demonstrate that Kin1 and Kin2 induce phosphorylation of Sec9 and its release from the plasma membrane, which, presumably, promotes incorporation of Sec9 into novel SNARE complexes. We further find that the conserved 42-amino acid tail of the yeast Par-1 ortholog plays a role in the autoinhibition of the kinase function in the secretory pathway of *S. cerevisiae*.

MATERIALS AND METHODS

Media and Reagents

Yeast cells were grown in either YP medium (1% bacto-yeast extract, 2% bacto-peptone; Difco, Detroit, MI), S medium (0.67% yeast nitrogen base; Difco), or SC medium (0.67% yeast nitrogen base with dropout selection-appropriate amino acid nutrients) supplemented with 2% glucose or 1% galactose. Sorbitol, sodium azide, sodium fluoride, *N*-ethylmaleimide, β -mercaptoethanol, Triton X-100, and protease inhibitors were obtained from Sigma-Aldrich (St. Louis, MO). Zymolase (100T) was purchased from Seikagaku (Tokyo, Japan). ¹²⁵I-Protein A and [³²P]ATP, ³⁵S-TransLabel, [³⁵S]methionine, and [³²P]orthophosphate were obtained from PerkinElmer Life and Analytical Sciences (Boston, MA) and protein A-Sepharose CL-4B from Amersham Biosciences (Piscataway, NJ). Molecular weight markers and Tween 20 were from Bio-Rad (Hercules, CA). Restriction enzymes, calf intestinal phosphatase, and λ -phosphatase were purchased from New England Biolabs (Beverly, MA).

Yeast Genetic Techniques

Transformations were performed using the lithium acetate method (Becker and Guarente, 1991). Crosses of strains, tetrad dissection, and diploid sporulation were performed as described previously (Guthrie, 1991).

Antibodies

Rabbit antisera were raised against glutathione *S*-transferase (GST)-fusion proteins containing residues 852-1032 of the C terminus of Kin1 and containing residues 964-1121 of the C terminus of Kin2 (Cocalico Biologicals, Reamstown, PA). Antibodies were affinity purified as described previously (Lehman *et al.*, 1999).

Plasmid Construction and Generation of Mutants

Constructs were generated by polymerase chain reaction (PCR) amplification by using primers (QIAGEN Operon, Alameda, CA) incorporating appropriate restriction sites. Primers were designed to incorporate ~1000 base pairs upstream of the open reading frame (ORF) and 250 base pairs downstream of the stop codon into the construct. *SalI/EcoRI* sites were used to subclone full-length *KIN1* into the pRS426 vector. To generate *KIN2* constructs, *KIN2* (1-1147), *kin2-CT* (521-1147), *KIN2-NT* (1-526), *kin2-KD* (K128M), *KIN2-Δ42* (1-1106), and 800 base pairs of the sequence upstream of the ORF were introduced into pRS426 as a *NotI/EcoRI* segment, and subsequently, wild-type and mutant *KIN2* ORF sequences were subcloned into the same vector by using *EcoRI/XhoI* sites. Fusion PCR technique was used to generate *KIN2-NT*, *KIN2-Δ42*, and *kin2-KD*. For the fusion reaction, segments with overlapping sequences generated in the first round of the amplification were resolved on 1.5% low-temperature agarose gel, cut out, and used as templates in the second round of the PCR amplification. Catalytic domains of *SNF1*, *HSL1*, *GIN4*, *KCC4*, *YPL141C*, *KIN4*, and *YPL150W* were mapped by BLAST sequence alignment with *KIN2*. *NotI/XhoI* sites were used to subclone *HSL1* (1-462), *GIN4* (1-432), *KCC4* (1-437), *YPL141C* (1-387), and *YPL150W* (1-426) into pRS426 vector. *NotI/SalI* sites were used to subclone *SNF1* (1-432) and *KIN4* (1-366) into the pRS426 vector. Galactose-inducible *KIN1* and *KIN2* constructs were generated by insertion of PCR-amplified fragments behind the *GAL* promoter of *GAL/HIS/CEN* (*BamHI/SalI* sites used) and *GAL/LEU/CEN* (*BamHI/XhoI* sites used) vectors, respectively. Generation of high copy *SEC9* construct and Sec9-CT (402-651) GST-fusion protein were described elsewhere (Rice *et al.*, 1997). Sec9-NT1 (1-168) and Sec9-NT2 (166-401) GST-fusion proteins were obtained by subcloning Sec9-NT1 and Sec9-NT2 into the *BamHI/SalI* and *BamHI/EcoRI* sites, respectively, of the pGEX4T1 vector (Amersham Biosciences). The Sec9-NT2-S315A mutant was created by fusion PCR via mutation-incorporating primers. All mutants were verified by sequencing. Generation of GST-*KIN2* kinase domain (1-520) construct was obtained by subcloning a PCR-generated fragment containing *kin2-NT* (1-520) into the *BamHI-XhoI* sites of the pGEX4T1 vector. The C-terminal Kin2 fragments *kin2-CT* (523-1147) and *kin2-CTΔ42* (523-1106) were placed under the control of a T7 promoter for transcription and translation by PCR amplification. The upstream oligo was designed for translation beginning at residue 532 in the *KIN2* coding sequence. The downstream oligo was designed to

anneal ~40 base pairs distal to the stop codon of *KIN2*. PCR products for coupled translation/transcription were generated using templates containing either *KIN2* or *KIN2-Δ42* mutant. Translation of each PCR product resulted in a radiolabeled protein of the expected size on SDS-PAGE.

Suppression Assays

Late *sec* mutant cells were transformed with high copy plasmids (e.g., vector, *KIN1*, and *KIN2*) or a galactose-inducible *Kin2* construct (vector and *GALKIN2*) and grown on selective medium, picked into microtiter plates, and replica plated onto YP-D medium (YP supplemented with 2% glucose) or YP-Gal (YP supplemented with 1% galactose). Transformants were tested for growth at permissive (25°C) and restrictive (14, 33, 35, and 37°C) temperatures.

Two-Hybrid Analysis

ORFs of *kin2-CT* (521-1147) and *kin2-CTΔ42* (521-1106) were subcloned as N-terminal fusion fragments into *NcoI/BamHI* sites of pAS1-CYH2 *GAL4*-binding domain vector (BD). ORFs of *KIN2* (1-1147), *KIN2-NT* (1-526), *kin2-CT* (521-1147), *KIN2-FLΔ42* (1-1106), and *kin2-CTΔ42* (521-1147) were inserted as N-terminal fusion fragments into *NcoI/BamHI* sites of pACT2 *GAL4*-activation domain vector (AD). Constructs were transformed into the PJ694 α strain containing *GAL4*-inducible *HIS3* and *ADE* reporter genes. Construct expression was verified by Western blotting. Transformants expressing interacting proteins gained the ability to grow on -His and -Ade media. As a control empty BD and AD vectors were analyzed for the interaction with each AD and BD fusion construct, respectively. Only signals detected in the absence of control background were considered positive.

In Vitro Binding Assays

PCR generated fragments containing *kin2-CT* (523-1147) and *kin2-CTΔ42* (523-1106) were placed under control of a T7 promoter and in vitro transcribed and translated using a coupled reticulocyte lysate transcription/translation system (TnT; Promega, Madison, WI) in the presence of [³⁵S]methionine. The radiolabeled proteins were diluted in binding buffer (10 mM HEPES-KOH, pH 7.4, 140 mM KCl, 2 mM MgCl₂, 0.5% Triton) with GST-Kin2 kinase domain (present at ~1 μ M) for 1 h at 4°C. Supernatant and pellet fractions were separated and run on a 7% gel, dried, and exposed to film. Binding of radiolabeled proteins was quantified using the PhosphorImager screen and STORM ImageQuant software (Amersham Biosciences).

Construction of Deletion Strains

Gene disruption was performed via homologous recombination. Initially, flanking sequences upstream and downstream of the target ORF were introduced into the integration vector, respectively, upstream and downstream of the coding sequence of the appropriate selection marker. Plasmids were linearized before the transformation. The *KIN1* gene was disrupted by the insertion of the *LEU2* marker via pRS305 *LEU2* vector. *KIN2* gene was disrupted by the insertion of the *HIS3* marker via pRS303 *HIS3* vector. The genotype of the yeast strain transformed with these constructs was MAT a/ α ; *ura3-52/ura3-52*; *leu2-3112/leu2-3112*; *his3-Δ200/his3-Δ200*. Diploids were selected on either -His or -Leu medium and sporulated. Tetrads were dissected and analyzed for the presence of the selective markers and the viability at different temperatures. Disruption was confirmed by PCR and immunoblotting with α -Kin1 and α -Kin2 antibodies. Crossing of the single *kin1Δ* and *kin2Δ* deletion strains generated a strain with the double deletion *kin1Δ, kin2Δ*, which was analyzed in a similar manner. The *SNF1* gene was disrupted using a purified PCR product containing *SNF1* sequences flanking the Kanamycin gene (*snf1Δ::Kan^R*), which was transformed into the wild-type strain and in the strain homozygous for the *KIN1* deletion and heterozygous for the *KIN2* deletion: MAT a/a; *kin1Δ::LEU2/kin1Δ::LEU2*; *KIN2/kin2Δ::HIS3*; *leu2-3112/leu2-3112*; *his3-Δ200/his3-Δ200*; *ura3-52/ura3-52* to create the triple deletion mutant *kin1Δ, kin2Δ, snf1Δ*. YPD-G418 plates were used for the selection of the Kan^R-containing transformants. Diploids were sporulated, and tetrads were analyzed for marker distribution. Generation of the triple mutant *kin1Δ, kin2Δ, snf1Δ* was confirmed by PCR.

Subcellular Fractionation

Procedure was described in detail previously (Lehman *et al.*, 1999). Three strains were used: vector only (pRS426), *KIN1* on high copy vector, and *KIN2* on high copy vector. Cells were washed, spheroplasted, lysed, and divided into two pools, which were subjected to the differential treatment with or without Triton X-100 and centrifuged at 30,000 \times g. Supernatant and pellet fractions were isolated and normalized for further analysis. Samples boiled in SDS sample buffer were subjected to 7% SDS-PAGE and blotted with affinity-purified antibodies to Kin1, Kin2, and Sso1/2. Signal was quantified using the PhosphorImager screen and STORM ImageQuant software (Amersham Biosciences).

BglIII Secretion Assays

Secretion assays examining the effect of multicopy *KIN2* were performed on *sec15-1* mutant cells (*ura3-52; sec15-1*) transformed with *KIN2* on a high copy vector or vector only (pRS426). Cells were grown overnight at 25°C and then shifted to 36°C for 1 h. Cells were then processed for BglIII secretion as described previously (Adamo *et al.*, 1999). Secretion assays on *GAL* induced *KIN1* were performed on *sec1-1* mutant cells (*GAL+*, *ura3-52; leu2-3112; his3-Δ200; sec1-1*) containing vector only (*GAL/LEU2*) or galactose inducible *KIN1* on *GAL/LEU2* integrative vector as well as a wild-type control strain. Cells were grown overnight to an OD₅₉₉ = 0.5 in YP-raffinose (3%) medium at 25°C and then induced with 1% galactose for 2 h before shifting the cells to 33°C for 2 h. Cells were then processed for BglIII secretion as described previously (Adamo *et al.*, 1999).

Native Immunoprecipitation

Cells from strains containing either high copy *KIN1*, *KIN2*, or vector alone were grown O/N in SC-D medium to OD₅₉₉ = 0.5 and then shifted for 2 h to grow in YP-D medium at 25°C to OD₅₉₉ = 1 to the total of 266 OD units. Subsequently, cells were harvested, washed in ice-cold 10:20:20 buffer (10 mM Tris, 20 mM sodium azide, 20 mM sodium fluoride), and spheroplasted in 17.8 ml of spheroplast buffer (100 mM Tris, 20 mM sodium azide, 20 mM sodium fluoride, 1.2 M sorbitol, 21 mM β-mercaptoethanol, 0.1 mg/ml 100T Zymolyase) for 30 min at 37°C. Spheroplasts were lysed in 8.8 ml of ice-cold lysis buffer (20 mM HEPES-KOH, 150 mM KCl, 0.5% IGEPAL) with protease inhibitors (PIC): 2 mM 4-(2-aminoethyl)benzenesulfonyl fluoride, 1 mM phenylmethylsulfonyl fluoride, 20 μM Pepstatin A, 2 μg/ml leupeptin, aprotinin, and antipain. The insoluble material was pelleted by 10-min spin in a 4°C Microfuge, and the supernatant was used to set up immunoprecipitation (IP) reactions (1 ml/1 IP). Saturating amounts of affinity purified antibodies to Kin1 and Kin2 were incubated with the lysate for 1.5 h on ice. In parallel, control IPs were set up with equal amounts of purified preimmune IgG. Next, protein A-Sepharose was added to the lysates (60 μl of 1:1 suspension per IP), and tubes were placed on a nutator for 1 h. Beads were washed four times with lysis buffer and boiled in 100 μl of sample buffer. Samples were subjected to SDS-PAGE, transferred to the nitrocellulose membrane, and immunoblotted with polyclonal antibodies to Kin1, Kin2, Sec9, and Sro7 followed by I¹²⁵-protein A secondary.

Dithiosuccinimidylpropionate (DSP) Cross-linking

Strains containing high copy *SEC9* and high copy *KIN1* were grown overnight in SD (S medium with 2% glucose). Six OD units of cells were labeled with [³⁵S]methionine and cysteine in 4 ml for 1 h at 30°C. Cross-linking and immunoprecipitation were performed as described previously (Lehman *et al.*, 1999). Labeled cells were washed in phosphate-buffered saline (PBS)-azide, spheroplasted in 1 ml of spheroplast buffer, and lysed in 300 μl of PBS with PIC. The lysate was divided into two pools, one treated with the chemical cross-linker DSP dissolved in dimethyl sulfoxide (DMSO), and the control pool was treated with DMSO only. The cross-linker was quenched by ammonium acetate, samples were boiled in 5× boiling buffer (5% SDS, 50 mM Tris, pH 8.0, 25 mM EDTA) and diluted 20× with IP buffer (10 mM Tris, pH 8, 150 mM NaCl, 0.5% Tween 20, 0.1 mM EDTA). Cell lysates were then subjected to two rounds of IPs. First, samples from both pools were incubated with affinity-purified antibodies to α-Kin1, α-Sec9, and preimmune IgG overnight at 4°C. Immune complexes were pooled via protein A-Sepharose. For the second round of IPs beads were resuspended in the reducing boiling buffer (1% SDS, 10 mM Tris, pH 8.0, 5 mM EDTA, 0.1 mM dithiothreitol [DTT]), boiled, diluted with IP buffer, and supernatants were subjected to IPs with either affinity-purified α-Kin1 or affinity-purified α-Sec9 antibodies. Samples were boiled and resolved on 7% SDS-PAGE, and a ³⁵S signal was detected by autoradiography.

Nonnative Immunoprecipitation and Phosphatase Treatment

Yeast strains containing high copy *SEC9* and either inducible *KIN2* on *GAL/LEU/CEN* integrative vector or *GAL/LEU/CEN* empty vector were grown in SC medium with 3% raffinose overnight and induced with 1% galactose for 4 h at 25°C. Then, 100 OD units/each were harvested, washed, spheroplasted in Eppendorf tubes (5 OD/tube), and lysed in 40 μl/tube TEAE/sorbitol (10 mM triethanolamine, 1 mM EDTA, pH 7.2, 0.8 M sorbitol with 1× protease inhibitor mix). Lysates were centrifuged, combined with an equal volume of 2× boiling buffer (10 mM Tris, pH 8.0, 25 mM EDTA pH 8.0, 1% SDS), boiled at 95°C for 5 min, and diluted 20× with IP buffer (10 mM Tris, pH 8.0, 150 mM NaCl, 0.1 mM EDTA, 0.5% Tween 20). Combined supernatants were distributed into Eppendorf tubes (1.4 ml/tube) and immunoprecipitated with antisera to Sec9 (6 μl/tube) overnight on ice. Immune complexes were pooled down with protein A-Sepharose (65 μl/tube) for 2 h at 4°C and washed with IP buffer five times. Combined beads were distributed into Eppendorf tubes (25-μl bed volume/tube), which were subjected to five treatments: 1) boiled immediately; 2) incubated 1:1 with 2× restriction buffer 3 and 2 μl/tube of calf intestinal phosphatase (CIP) for 30 min at 37°C; 3) incubated with 2× buffer 3 only for 30 min at 37°C (mock control for CIP); 4) incubated 1:1 with

2× λ-phosphatase buffer and λ-phosphatase (1.5 μl/tube) for 30 min at 30°C; and 5) incubated with 2× λ-phosphatase buffer only for 30 min at 30°C (mock control for λ-phosphatase). Samples were boiled, separated on an 8% gel, and immunoblotted with α-Sec9 antibody.

Purification of the Recombinant Proteins

All GST-fusion proteins were produced, purified, and their protein concentrations estimated as described previously (Rossi *et al.*, 1997).

In Vitro Kinase Assays

Yeast strains containing high copy *KIN1*, *KIN2*, or empty vector were grown on SC-D (SC medium with 2% glucose) overnight and switched to YP-D medium for 2.5 h. Cells were harvested (33 OD units/1 IP reaction), washed in 10:20:20 buffer, spheroplasted, lysed, and subjected to native immunoprecipitation with antibodies to Kin1, Kin2, or preimmune serum as described above. Immune complexes were pulled down with protein A-Sepharose (60 μl of 1:1 slurry/1 IP), beads were washed twice with lysis buffer and twice with PK buffer (50 mM Tris, pH 7.5, 5 mM MgCl₂), and combined and distributed into Eppendorf tubes. For one kinase reaction (total volume of 50 μl), we used 25 μl of 1:1 bead slurry, 1.5 μM recombinant protein, 1× PKi buffer (50 mM Tris, pH 7.5, 5 mM MgCl₂, 1 mM DTT), 0.1 mM cold ATP, and 1 μl of [³²P]ATP. The kinase reaction was incubated at 30°C for 30 min, spun, and the supernatant containing recombinant proteins was boiled in an equal volume of sample buffer. Samples were subjected to 15% SDS-PAGE, and gels were dried and exposed to film.

In Vivo Kinase Assays

Cells containing multicopy *SEC9* and *GAL-KIN2* (*GAL-KIN2/CEN/LEU2*) or empty vector control (*GAL/CEN/LEU2*) were grown O/N in S medium with 3% raffinose to an OD₅₉₉ of 0.5. Next day the cells were split in half and shifted into fresh medium containing either S with 2% raffinose or YP-low phosphate with 2% raffinose for 1 h at 27°C. Two ODs of the culture grown in S with 2% raffinose were then induced with 1% galactose and labeled with [³⁵S]methionine (0.28 μCi/ml) for 4 h at 27°C. 2 ODs of the culture growing in YP-low phosphate with 2% raffinose were simultaneously induced with 1% galactose in the presence of [³²P]orthophosphate (10 μCi/μl) for 4 h at 27°C. At the end of the incubation, the cultures were spun in glass tubes for 5 min at 25°C. All samples were washed in Tris (10 mM), sodium azide (20 mM), and sodium fluoride (20 mM) and then spheroplasted in spheroplast buffer (100 mM Tris, 1.2 M sorbitol, 10 mM sodium azide, 0.015% β-mercaptoethanol, 0.1 mg/ml Zymolyase 100T) for 30 min at 37°C. Subsequently, samples were spun in Eppendorf tubes for 5 min at 2000 rpm. The pellets were lysed in 75 μl of ice-cold 1× PBS and then boiled immediately in 2× boiling buffer (2% SDS, 20 mM Tris, pH 8, 10 mM EDTA) for 5 min at 95°C. Samples were diluted with 1 ml of IP buffer (10 mM Tris, pH 8, 150 mM NaCl, 0.5% Tween 20, 0.1 mM EDTA), and microfuged for 10 min at 4°C. Supernatants were then removed, further diluted in IP buffer, and used for immunoprecipitations with respective antibodies for 1 h on ice. For [³²P]orthophosphate-labeled cells, RNase A (DNase, protease free; Sigma-Aldrich) was added to 30 μg/ml (1 μl of enzyme/ml IP buffer) to reduce background on gels from radiolabeled RNA contaminants. Immune complexes were pulled down with protein A-Sepharose, washed with IP buffer, and IP buffer with 2 M urea and 1% betamercaptoethanol before boiling in 100 μl of SB. Samples were run on SDS polyacrylamide gels, dried, and exposed to film.

RESULTS

KIN1 and *KIN2* Are Potent Suppressors of Secretion-defective Alleles of *Rho3* and *Cdc42*

Rho3 is a member of the Rho family of GTPases that exhibits multiple genetic and physical interactions with components of the exocytic machinery and is itself required for efficient exocytosis (Adamo *et al.*, 1999; Robinson *et al.*, 1999). To isolate candidate downstream effectors of *RHO3* function in exocytosis, we performed a genetic screen for dosage suppressors of the slow growth phenotype of a *RHO3* deletion strain (*rho3Δ*). We constructed a strain containing the *RHO3* coding sequence under the control of the glucose-repressible *GAL* promoter as the only source of *Rho3* in the cell. This strain, which grows normally on galactose-containing media but extremely slowly in glucose-containing media, was transformed with a yeast genomic library prepared in a multicopy vector, and transformants were selected for growth on glucose-containing medium. Plasmids from colonies growing on glucose were isolated, retested for suppression, and then analyzed by sequencing. From this anal-

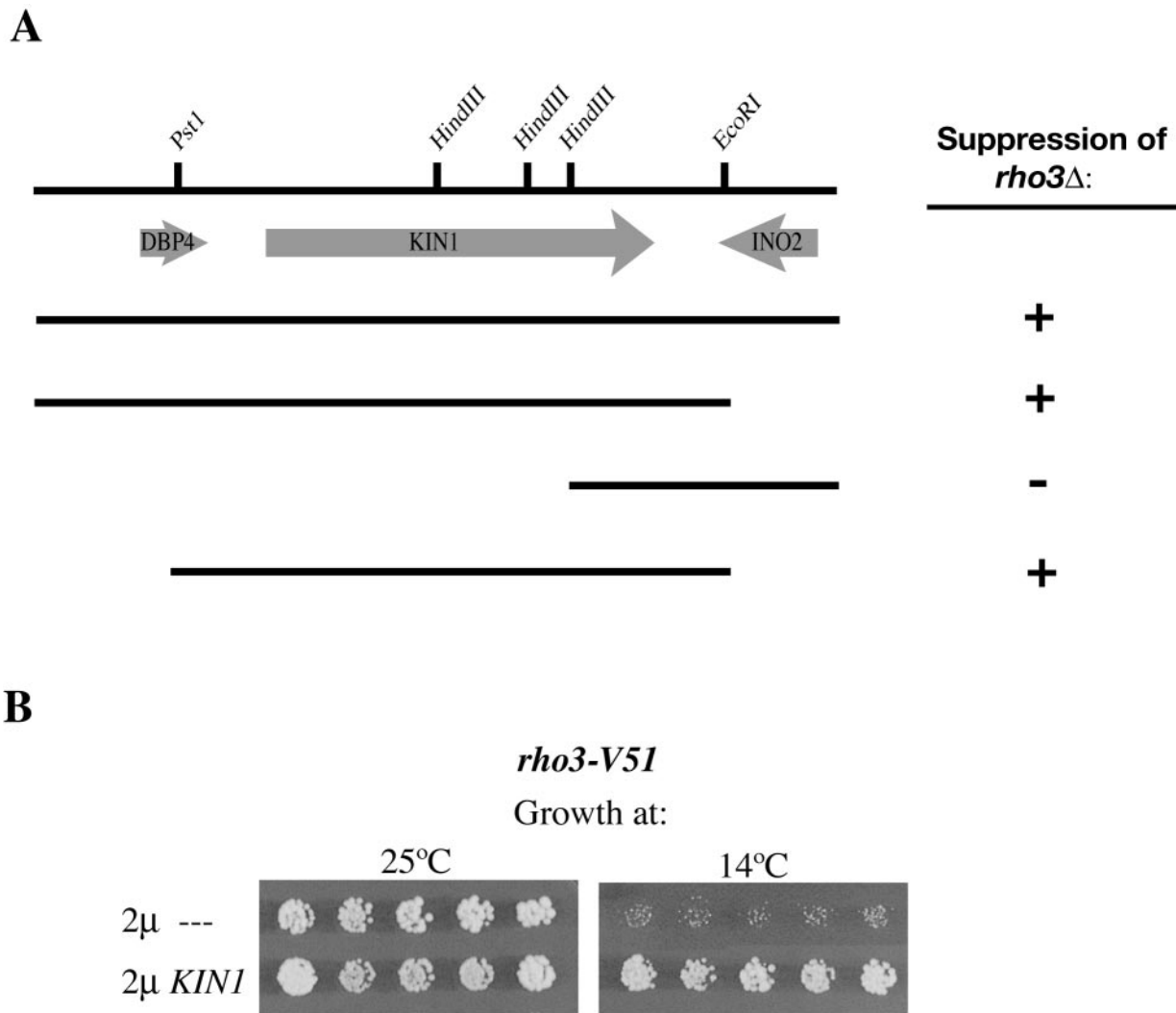


Figure 1. Isolation of *KIN1* as a suppressor of the *RHO3* deletion (*rho3Δ*). (A) Scheme shows genomic DNA fragments identified as suppressors of the *rho3Δ* phenotype. Cells containing a single copy of the galactose-inducible *RHO3* were transformed with a genomic library on a high copy vector and cultured in the presence of 2% glucose to repress *Rho3* expression. Plasmids from transformants exhibiting normal growth in the absence of *RHO3* were isolated and sequenced. The open reading frame of *KIN1* alone was shown to be sufficient for the full suppression of *rho3Δ*. (B) *KIN1* suppresses the cold sensitivity of the *rho3-V51* mutant. The *rho3-V51* mutant was transformed with *KIN1* on a multicopy plasmid, cultured on selective media at 25°C, replica plated from the microtiter plates to YPD media, and incubated at permissive (25°C) and restrictive (14°C) temperatures.

ysis, we identified 25 suppressing plasmids containing overlapping parts of six distinct loci. Five of the six loci had genes previously isolated as dosage suppressors of a *rho3Δ* mutant: *BEM1* (1 isolate), *SRO9* (1 isolate), *SEC4* (2 isolates), *SSO2* (3 isolates), and *RHO3* itself (17 isolates) (Imai *et al.*, 1996; Adamo *et al.*, 1999). Subcloning of the various regions in the sixth locus identified the suppressing gene to be coincident with the *KIN1* gene (Figure 1A). Although several suppressors of *rho3Δ* (*SEC4*, *SRO7*, *SRO77*, *SEC9*, and *SSO2*) are known components of the late secretory machinery, the function of *KIN1* is not known. The *KIN1* open reading frame alone was sufficient to suppress *rho3Δ*, and thus we identified *KIN1* as a novel dosage suppressor of *Rho3*.

Mutations in *RHO3* affect both actin organization and post-Golgi vesicle transport (Imai *et al.*, 1996; Adamo *et al.*, 1999). The *rho3-V51* cold-sensitive mutant has a secretory defect in the absence of functional and structural perturbations of the actin cytoskeleton; hence, this mutant affects a

function of *Rho3* in exocytosis that is independent of actin (Adamo *et al.*, 1999). To determine whether *Kin1* functions specifically in the secretory pathway downstream of *Rho3*, we assessed the ability of *KIN1* to suppress the *rho3-V51* mutant. *rho3-V51* is viable at 25°C, but not at 14°C. Figure 1B shows that overexpression of *KIN1* resulted in restoration of growth of the *rho3-V51* mutant at the restrictive temperature (14°C). In addition, we have previously reported that the growth defect of *cdc42-6*, the secretion-impaired mutant of another *Rho* GTPase, is specifically suppressed by introduction of *KIN1* on the multicopy plasmid (Adamo *et al.*, 2001). This suppression was specific to *cdc42-6*, because *KIN1* failed to suppress more pleiotropically defective alleles of *CDC42* such as *cdc42-1*.

Because the coding sequence of *KIN2* is similar to that of *KIN1* (51% identity), we asked whether they shared a common function downstream of *Rho3* and *Cdc42* by determining the ability of high-copy *KIN2* to suppress the growth

Table 1. *KIN1* and *KIN2* act redundantly in suppression of *rho3-V51* and *cdc42-6*, secretion-impaired mutants of Rho GTPases

Mutant	2 μ <i>KIN1</i>	2 μ <i>KIN2</i>	2 μ vector
<i>rho3-V51^{cs-}</i>	+++	+++	—
<i>cdc42-6^{ts-}</i>	+++	+++	—

rho3-V51 and *cdc42-6* mutants were transformed with either vector (pRS426), *KIN1*, or *KIN2* on high copy, cultured on selective medium at room temperature, and replica plated from the microtiter plates to YP-D media. Growth of transformants at mutant's restrictive temperatures, 14° C for *rho3-V51* and 32° C for *cdc42-6*, was tested. Scoring reflects the colony growth at restrictive temperatures relative to the wild-type yeast (+++) and to the empty vector control (—).

defects associated with *rho3-V51* and *cdc42-6* mutant strains. As shown in Table 1, we found that *KIN2* strongly suppressed the growth defect of these mutants at their respective restrictive temperatures (14°C for *rho3V-51* and 32°C for *cdc42-6*), and the potency of *KIN2* was identical to that of *KIN1*. The fact that both kinases specifically suppress secretory-defective alleles of Rho3 and Cdc42 suggests that both *KIN1* and *KIN2* act in the secretory pathway downstream of the Rho GTPases.

KIN1 and *KIN2* Exhibit Genetic Interactions with Components of the Late Secretory Machinery

The ability of *KIN1* and *KIN2* to suppress the *cdc42-6* and *rho3-V51* alleles suggests a possible role for these kinases in the regulation of exocytosis. To further explore this idea, we examined the ability of multicopy *KIN1* and *KIN2* to suppress the temperature-sensitive growth defect of a number of secretory (*sec*) mutants. An example of the suppression analysis, summarized in Table 2, is shown in Figure 2. Elevated dosage of *KIN1* and *KIN2* restored the growth of

Table 2. Summary of late *sec* mutants suppression by *KIN1* and *KIN2*

Mutant	2 μ <i>KIN1</i>	2 μ <i>KIN2</i>
<i>sec1-1^{ts-}</i>	+	+
<i>sec2-41^{ts-}</i>	++	++
<i>sec3-2^{ts-}</i>	+/-	+/-
<i>sec4-P48^{cs-}</i>	+++	+++
<i>sec5-24^{ts-}</i>	—	—
<i>sec6-4^{ts-}</i>	—	—
<i>sec8-9^{ts-}</i>	—	—
<i>sec9-4^{ts-}</i>	—	—
<i>sec10-2^{ts-}</i>	++	++
<i>sec15-1^{ts-}</i>	+++	+++

Late acting *sec* mutants were transformed with either vector (pRS426), *KIN1*, or *KIN2* on high copy. Growth of transformants at restrictive temperatures was tested. *sec* mutants restrictive temperatures are as follows: 33°C for *sec1-1*, 33°C for *sec2-41*, 35°C for *sec3-2*, 14°C for *sec4-P48*, 33°C for *sec5-24*, 35°C for *sec6-4*, 37°C for *sec8-9*, 34°C for *sec9-4*, 35°C for *sec10-2*, and 35°C for *sec15-1*. Scoring reflects the mutant colony growth at their respective restrictive temperatures relative to the wild-type yeast (+++) and empty vector control (—). Suppression of the *sec* mutants is indicated as follows: +++, very strong; ++, strong; +, moderate; and +/-, weak.

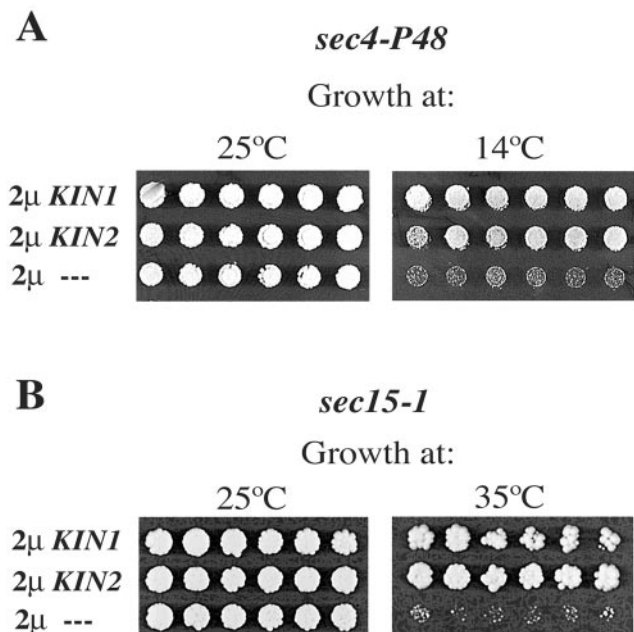


Figure 2. *KIN1* and *KIN2* suppress late secretory mutants. *KIN1* and *KIN2* suppress the cold sensitivity of the *sec4-P48* mutant (A) and the temperature sensitivity of the *sec15-1* mutant (B). Mutants were transformed with *KIN1* and *KIN2* on high copy plasmids, cultured on selective media at 25°C, replica plated from the microtiter plates to YPD media, and incubated at restrictive (14°C for *sec4-P48* and 35°C for *sec15-1*) and permissive (25°C) temperatures.

the late *sec* mutants *sec4-P48* and *sec15-1* to wild-type levels at 14 and 35°C, respectively (Figure 2). *sec4-P48* is a cold-sensitive effector domain mutant of the Rab GTPase *SEC4* (Brennwald *et al.*, 1994), whereas *sec15-1* is a temperature-sensitive mutant of one of the components of the Exocyst complex, Sec15 (TerBush and Novick, 1995). We examined the secretory defect in *sec15-1* cells with multicopy *KIN2* compared with control *sec15-1* cells containing empty vector after a shift to the restrictive temperature. This analysis demonstrated that although unsuppressed *sec15-1* cells are found to accumulate 36% of *BglIII* internally, the accumulation is reduced to wild-type levels in *sec15-1* cells containing high-copy *KIN2* where only 18% of *BglIII* is found internally. Therefore, the suppression of the growth defect was found to correlate closely to suppression of the secretion defect in these cells. Suppression analysis demonstrated that *KIN1* and *KIN2* also suppress the growth defect of a number of other late secretory mutants. These include the temperature-sensitive mutants of two additional components of the Exocyst complex; Sec3 (*sec3-2*) and Sec10 (*sec10-2*), which were rescued at the nonpermissive temperature of 35°C by introduction of *KIN1* and *KIN2* on high copy. Also, we show that expression of multicopy *KIN1* and *KIN2* restores the growth of *sec1-1* at 33°C and *sec2-41* at 33°C. *sec1-1* is a mutant of *SEC1*, which is involved in SNARE assembly (Carr *et al.*, 1999), and *sec2-41* is a mutant in *SEC2*, the nucleotide exchange factor for Sec4 (Walch-Solimena *et al.*, 1997). Thus, *KIN1* and *KIN2* exhibit strong genetic interactions with multiple components of the exocytic machinery. The suppression profile of *KIN1* was identical to that of *KIN2*, providing additional evidence in favor of the functional redundancy of the two kinases (Table 4). The ability of *KIN1* and *KIN2* to suppress several late *sec* mutant genes indicates that they

function downstream of these proteins at the later stage of exocytosis.

However, we found that *KIN1* and *KIN2* do not suppress the temperature-sensitive phenotype of the *sec9-4* mutant (Table 2), a mutant of the t-SNARE Sec9 that is defective in SNARE complex assembly and that is required for vesicle fusion with the plasma membrane (Rossi *et al.*, 1997), nor do they suppress the growth defect of *sro7/77Δ*, a mutant with a double disruption of genes encoding Sec9-binding proteins Sro7 and Sro77 (Table 4). These observations place Kin1 and Kin2 function downstream of polarized vesicle delivery and upstream of the terminal fusion event.

Analysis of the Structural Requirements for *KIN1* and *KIN2* Function in the Secretory Pathway

To elucidate the nature of Kin1 and Kin2 function in the secretory pathway, we determined the minimal domain requirement that confers suppression. Kin1 and Kin2 contain a kinase domain at the N terminus of the protein and a regulatory domain at the C terminus (Figure 3A). The kinase domain as well as the 42-amino acid stretch on the extreme carboxy terminus are highly conserved between Kin1 and Kin2 and a number of their orthologues from other species. Because Kin1 and Kin2 proteins display structural and functional redundancy, we focused on Kin2. Mutant *KIN2* constructs with deletions of the kinase domain or the 42 amino acid C-terminal tail were designed to assess the significance of these domains for Kin2 function in the secretory pathway. The following mutants were generated: *KIN2-NT*, lacking the regulatory C-terminal domain of the protein; *kin2-CT*, lacking the catalytic N-terminal domain; *kin2-KD*, the kinase-dead mutant, where a single critical Lys¹²⁸ residue in the second catalytic domain (conserved residue mapped by kinase sequences alignment; Hanks *et al.*, 1988) was mutated to a Met; and finally the *KIN2-Δ42* mutant, with a deletion of the conserved 42 amino acid C-terminal tail (Figure 3A).

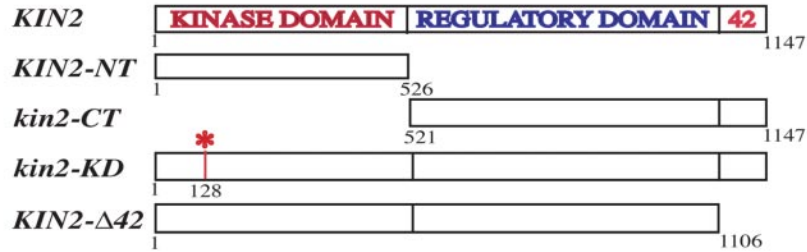
Function was assayed by analysis of the suppression properties of the *KIN2* mutants expressed at high copy. The suppression of the mutant phenotype of several late *sec* genes was tested, including *sec15-1* and *sec4-P48*, *sec1-1*, *sec2-41*, and *sec10-2* (Figure 3B). Wild-type *KIN2* on a multicopy plasmid behaved as reported above (Figure 2 and Table 2), restoring the viability of these mutants at certain restrictive temperatures. The kinase-inactive *KIN2* mutants *kin2-CT*, lacking the entire kinase domain, and *kin2-KD*, the kinase-dead mutant, failed to suppress the growth defect of all *sec* mutants tested (Figure 3B). These data demonstrate that the catalytic activity of Kin2 is critical for its function in the secretory pathway.

Multicopy expression of *KIN2-NT*, lacking the entire C-terminal domain, and *KIN2-Δ42*, lacking the 42 amino acid C-terminal tail, rescued the growth phenotype of all late *sec* mutants tested: *sec15-1*, *sec4-P48*, *sec1-1*, *sec2-41*, and *sec10-2* (Figure 3B). Thus, the regulatory domain of Kin2 is functionally dispensable. Furthermore, we observed that the *KIN2-NT* and *KIN2-Δ42* mutants at high copy gain the ability to suppress several secretory mutants: *sec1-1*, *sec2-41*, and *sec10-2*, at temperatures at which the wild-type *KIN2* failed to suppress (Figure 3B). The *sec1-1* and *sec2-41* temperature-sensitive mutants are suppressed at 33°C and the *sec10-2* mutant at 35°C in a comparable manner by *KIN2*, *KIN2-NT*, and *KIN2-Δ42* (our unpublished data). However, *KIN2* fails to suppress *sec1-1* at 35°C and *sec2-41* and *sec10-2* at 37°C, whereas the *KIN2-NT* mutant with the deletion of the regulatory domain is able to rescue these mutants at the more restrictive temperatures. Remarkably, the truncation of the distal 42 amino acids at the C terminus of *KIN2*, in *KIN2-Δ42*,

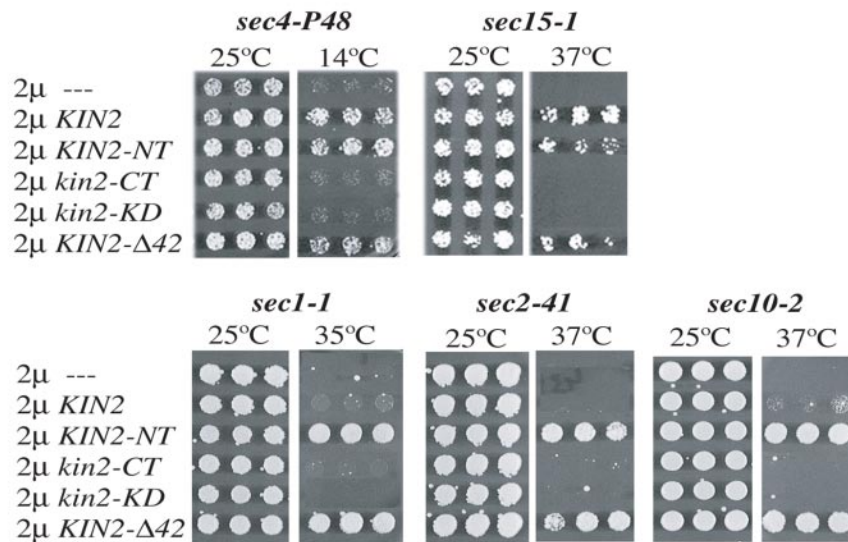
is sufficient to phenocopy the gain of function observed by *KIN2-NT*. Both mutant forms of *KIN2* are capable of suppressing *sec1-1* at 35°C and *sec2-41* and *sec10-2* at 37°C (Figure 3B). These data demonstrate that the C-terminal nonkinase domain of Kin2 acts as a negative regulator of Kin2 function in the secretory pathway and that the conserved 42-amino acid tail is essential for this negative regulatory function.

The greater potency of the Kin2 constructs lacking the distal C-terminal sequence might reflect the acquisition of the catalytically “active” protein conformation in the absence of the putatively inhibitory C-terminal tail. Possibly, in a dormant state the wild-type kinase exists in a closed conformation, with the tail bound to the catalytic core, hindering its activity, until the “ON” regulatory event relieves this autoinhibition (Figure 3C). This hypothesis presupposes the presence of a direct physical interaction between the tail of Kin2 and its kinase domain. To test whether this intramolecular interaction takes place, we used a yeast two-hybrid analysis. We created the following constructs: Kin2-CT and Kin2-CTΔ42 (encoding the regulatory domain with and without the C-terminal tail region, respectively) as GAL4 binding domain fusions and Kin2 (full-length protein), Kin2-NT (kinase domain), Kin2-CT (regulatory domain), Kin2-CTΔ42 (regulatory domain with the deletion of the C-terminal 42 amino acids) and Kin2-Δ42 (full-length protein with the deletion of C-terminal 42 amino acids) as GAL4 activation domain fusions. All constructs in activation and binding domain fusions were expressed at comparable levels as verified by Western blot analysis (our unpublished data). We found that the C-terminal regulatory domain of Kin2 (Kin2-CT in GAL4BD) binds to the catalytic N-terminal domain of Kin2 (Kin2-NT in GAL4AD) (Table 3). Moreover, this interaction is mediated by the conserved 42 amino acid tail, because it is abolished by truncation of the tail region in the C-terminal domain of Kin2: Kin2-CTΔ42 does not bind to Kin2-NT. Kin2-CT does not interact with itself, which is consistent with the regulatory domain interacting with the kinase domain only. In addition, although Kin2-CT fails to interact with the full-length Kin2, it shows interaction with the C-terminally truncated Kin2 Kin2-Δ42 (lacking the distal 42 amino acids). This result may signify that Kin2-CT associates with Kin2 in a presumably “open” or active conformation, as in Kin2-Δ42, but not with Kin2 in a closed conformation, as in full-length kinase. Thus, yeast two-hybrid analysis revealed that the regulatory domain of Kin2 binds to its catalytic domain and that the 42-amino acid tail is a prerequisite for this interaction. To further support the possible interaction of the Kin1/2 kinase domain with the C-terminal domain, we examined the ability of the domains to interact *in vitro*. We made use of a recombinant GST-fusion of the kinase domain and *in vitro*-translated C-terminal domain fragments containing either the intact C terminus, Kin2-CT(523–1147), or an identical domain lacking the conserved C-terminal 42 amino acids, Kin2-CTΔ42(523–1106). The results shown in Figure 3C demonstrate that these domains do in fact interact and that this interaction requires the C-terminal 42 residues of the Kin2. Together, the *in vitro* binding data and the two-hybrid analysis strongly suggest that the C-terminal regulatory domain of Kin2 physically interacts with the N-terminal kinase domain to mediate an autoinhibitory regulation of the kinase. Furthermore, we show that the highly conserved 42-amino acid tail of Kin2 is critical for the both the physical interaction between these domains and for the negative regulatory effect of the C-terminal domain as demonstrated by the effects on suppression of the late *sec* mutants. Together, this strongly suggests

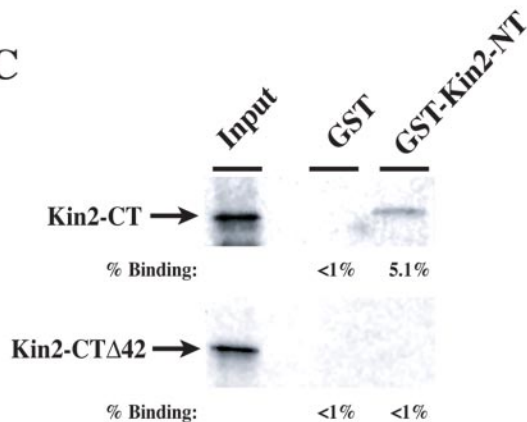
A



B



C



D



Figure 3. Analysis of the structural requirements for suppression of the secretory mutants by *KIN2*. (A) Schematic representation of the structure of Kin2 (conserved regions are indicated in red) and Kin2 mutants. Five constructs were examined. *KIN2*, wild-type; *KIN2-NT*, a mutant lacking the C-terminal domain; *kin2-CT*, a mutant lacking the kinase domain; *kin2-KD*, a kinase-dead mutant with a lysine to methionine substitution at residue 128 (the asterisk indicates the position of the point mutation); and *KIN2-Δ42*, a mutant with a deletion of the conserved 42-amino acid C-terminal tail. (B) Suppression assays show that the catalytic activity of Kin2 is essential for its function and that the conserved 42-amino acid tail plays a role in autoinhibition. Constructs described above along with the high copy vector control were transformed into *sec4-P48*, *sec15-1*, *sec1-1*, *sec2-41*, and *sec10-2* mutant strains, plated on YP-D media and cultured at permissive (25°C) and their respective restrictive temperatures. *kin2-KD* and *kin2-CT* failed to suppress the growth defect of all *sec* mutants tested. *KIN2-Δ42* and *KIN2-NT* exhibited suppression of *sec1-1* at 35°C and *sec2-41* and *sec10-2* at 37°C, whereas *KIN2* suppresses these mutants at 33°C only. (C) In vitro binding of Kin2 C terminus to the N-terminal Kin2 kinase domain demonstrates an intramolecular interaction that depends on the 42-amino acid tail. Kin2-CT or Kin2-CTΔ42 proteins (as shown in A) were in vitro translated in reticulocyte lysates and bound to GST fusion proteins immobilized on glutathione agarose beads. After binding, beads were washed, and the bound fraction was boiled in sample buffer and analyzed by SDS-PAGE and autoradiography. Input lane represents 10% of the radiolabeled protein. (D) Diagram depicting the proposed autoinhibitory intramolecular interaction between the N- and C-terminal domains of Par-1 family kinases.

Table 3. Yeast two-hybrid analysis shows that C-terminal 42 amino acid tail of Kin2 is necessary for the interaction of the regulatory C-terminal domain of Kin2 with the kinase domain

		Growth on	
BD-fusions	AD-fusions	–trp/–leu	–ade
Kin2-CT	Kin2	+++	—
	Kin2-NT	+++	+++
	Kin2-CT	+++	—
	Kin2-CTΔ42	+++	—
	Kin2-Δ42	+++	+++
Kin2-CTΔ42	—	+++	—
	Kin2	+++	—
	Kin2-NT	+++	—
	Kin2-CT	+++	—
	Kin2-CTΔ42	+++	—
	Kin2-Δ42	+++	—
	—	+++	—

GAL4BD-Kin2-CT (amino acids 521–1147) and GAL4BD-Kin2-CTΔ42 (521–1106) constructs were tested against GAL4AD-Kin2, GAL4AD-Kin2-NT (1–526), GAL4AD-Kin2-CT (521–1147), GAL4AD-Kin2-CTΔ42 (521–1106), and GAL4AD-Kin2-Δ42 (1–1106) constructs and vector containing GAL4AD alone (where GAL4BD is GAL4 binding domain vector; GAL4AD is GAL4 activation domain vector). Constructs were transformed into PJ694α strain, the presence of both activation and binding domain plasmids was confirmed by culturing on the selective medium (–trp/–leu), and an interaction was assayed by replica plating of six different colonies onto the medium lacking adenine (–ade). Protein expression was verified by Western blot analysis (our unpublished data). The full-length C-terminal domain of Kin2 in BD (GAL4BD-Kin2-CT) associates with AD-Kin2NT and AD-Kin2-Δ42 exclusively, and this association is abolished upon truncation of terminal 42 amino acids in GAL4BD-Kin2-CTΔ42.

that C-terminal domain of Kin1/2 functions as an autoinhibitory domain and that this autoinhibition requires the highly conserved C-terminal 42 amino acids. This provides the first mechanistic insight into to the function of this highly conserved 42-residue sequence at the C terminus of all Par-1 family kinases.

The Kinase Domain of SNF1, but Not Other Kinases of the CaMK Group, Show Suppression Properties of the Kin1 and Kin2 Kinases

It was previously reported that deletion of either *KIN1* or *KIN2* is neither lethal nor deleterious for cell growth (Lamb *et al.*, 1991; Donovan *et al.*, 1994). Because our data demonstrated functional redundancy of *KIN1* and *KIN2*, we proceeded to analyze whether the presence of at least one of these genes is required for cell viability. We created strains carrying single or double disruptions of these genes by homologous recombination. Consistent with the previous reports, *kin1Δ* and *kin2Δ* single disruptant strains were viable. The double disruptant *kin1Δ, kin2Δ* progeny, obtained by crossing of the *kin1Δ* strain with *kin2Δ*, demonstrate normal growth at all temperatures tested (25, 14, and 37°C). The single, *kin1Δ* and *kin2Δ*, and double *kin1Δ, kin2Δ* disruptants did not exhibit any significant defects in growth or secretion, as confirmed by invertase secretion assays (our unpublished data).

KIN1 and *KIN2* orthologues in *S. pombe*, *C. elegans*, *D. melanogaster*, and mammalian cells display pronounced gene disruption phenotypes. Hence, it is likely that in *S. cerevisiae* another molecule(s) acts to substitute the compromised func-

tion of Kin1 and Kin2. Kin1 and Kin2 belong to the CaMK protein kinase group, members of which share significant sequence similarity in the catalytic domain. Therefore, we examined whether other kinases of this group display functional redundancy with Kin1 and Kin2. BLAST search was used to identify the closest homologues of Kin1 and Kin2, and, as a result, we considered seven proteins of the CaMK group for further analysis, including Snf1, Hsl1, Gin4, Kcc4, Ypl141c, Kin4, and Ypl150w. To determine whether these proteins act in the secretory pathway, we tested their ability to rescue the growth defect of *sec2-41*, *sec10-2*, and *sec15-1*. Because several members of the CaMK group, such as Hsl1, Gin4, and Kcc4 bear a sequence at the distal carboxyl tail almost identical to that of Kin1 and Kin2, we hypothesized that they might be subjected to a similar mode of autoregulation as Kin2. To overcome this possible autoinhibition, we generated deletion constructs of *SNF1* (encoding amino acids 1–432), *HSL1* (1–462), *GIN4* (1–432), *KCC4* (1–437), *YPL141C* (1–387), *KIN4* (1–366), and *YPL150W* (1–426), which lack the regulatory domain while preserving intact all regions important for catalytic activity based on sequence alignment. These constructs were introduced on a multicopy plasmid into *sec15-1*, *sec10-2*, and *sec2-2* mutants and incubated at permissive and nonpermissive temperatures. We show that the catalytic domain of *SNF1* (*SNF1-NT*) suppresses the growth defect of *sec15-1*, *sec10-2*, and *sec2-2* mutants (Figure 4). Furthermore, the suppression of *sec* mutants by *SNF1-NT* is comparable to that of *KIN2-NT*. By contrast, constructs encoding the catalytic domains of Hsl1, Gin4, Kcc4, Ypl141C, Kin4, and Ypl150W failed to restore growth of the *sec* mutants at restrictive temperatures to any significant degree. Our data demonstrate that Snf1, which is structurally closer to Kin1 and Kin2 than any of the other seven members of the CaMK group, is the only kinase, out of those tested that may function redundantly with Kin1 and Kin2 in exocytosis.

To test whether the function of at least one of these genes, *KIN1*, *KIN2*, or *SNF1*, is essential for cell viability, we generated the strain with a triple disruption, *kin1Δ, kin2Δ, snf1Δ*. *kin1Δ, kin2Δ, snf1Δ* was created by substitution of *SNF1* with the *Kan^R* (Kanamycin) gene sequence in the context of the diploid strain homozygous for the *KIN1* deletion (*kin1Δ*) and heterozygous for the *KIN2* deletion (*kin2Δ*). A triple disruptant was obtained via sporulation and tetrad analysis. The triple mutant *kin1Δ, kin2Δ, snf1Δ* as well as the double *kin1Δ, snf1Δ*, and *kin2Δ, snf1Δ* mutants displayed slow growth phenotype inherent to the *SNF1* deletion alone (Celenza and Carlson, 1984). The *kin1Δ, kin2Δ, snf1Δ* triple mutant did not display any synthetic defect in growth or secretion (as verified by invertase secretion assays; our unpublished data).

Kin1 and Kin2 Physically Associate with Components of the Late Exocytic Machinery

Because genetic data place Kin1 and Kin2 function to the late secretory pathway, we analyzed whether these proteins physically associate with any of the components of the exocytic machinery.

Initially, we generated antibodies to detect Kin1 and Kin2 and characterized their localization in budding yeast. Antibodies were raised against a region in the C-terminal domain of Kin1 and Kin2. Affinity-purified antisera were tested by Western blot analyses on samples containing either high copy *KIN1* and *KIN2* or empty vector (Figure 5A). Kin1 and Kin2 antisera specifically recognized each protein and did not cross-react with the other gene product, with both proteins running on SDS-PAGE at ~145 kDa as predicted by the

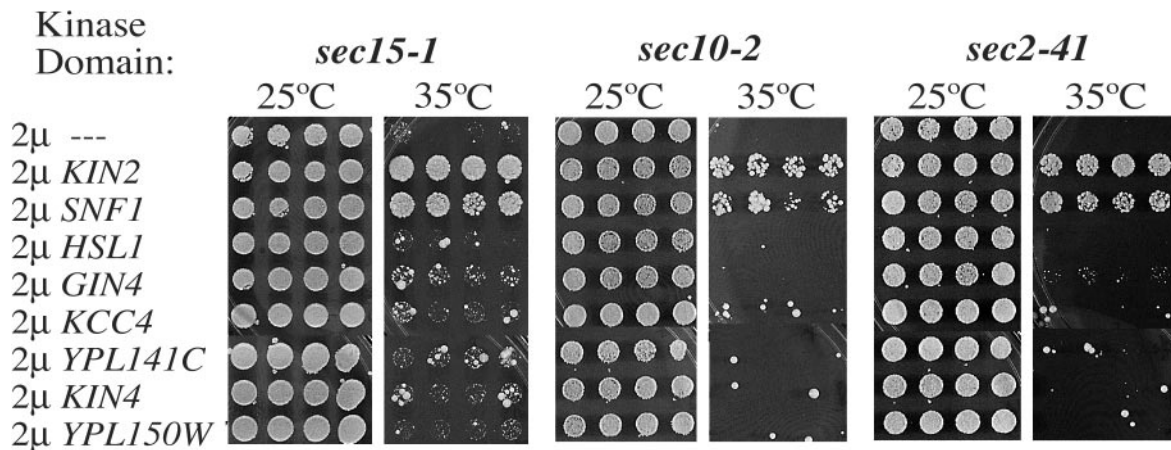


Figure 4. The catalytic domain of *SNF1*, but not of other kinases belonging to the Snf1 family, suppresses the same set of late secretory mutants as *KIN1* and *KIN2*. The *sec15-1*, *sec10-2*, and *sec2-41* mutants were transformed with either vector alone or the respective catalytic domains of *KIN2* (encoding residues 1–526), *SNF1* (1–432), *HSL1* (1–462), *GIN4* (1–432), *KCC4* (1–437), *YPL141c* (1–387), *KIN4* (1–366), and *YPL150w* (1–426) on high copy plasmids. Growth of transformants at respective restrictive temperatures was tested.

estimated molecular weight (Lamb *et al.*, 1991; Donovan *et al.*, 1994). Next, we analyzed the intracellular distribution of Kin1 and Kin2 by cell fractionation. Lysates from cells overexpressing Kin1 or Kin2 were treated with or without Triton X-100 and centrifuged at $30,000 \times g$. Supernatant and pellet fractions obtained were analyzed by SDS-PAGE and Western blot with anti-Kin1, anti-Kin2, and anti-Sso1/2 (as an internal control) antibodies (Figure 5B). We determined that ~70% of both Kin1 and Kin2 occur in the supernatant or cytosolic fraction (precisely 71.5% of Kin1 and 73.7% of Kin2 as an average of 3 or more experiments), and the remaining ~30% is found in the pellet or membrane-bound fraction. Therefore, consistent with the previous report (Tibbetts *et al.*, 1994), Kin1 and Kin2 partition to both cytosolic and membrane-associated pools in *S. cerevisiae*.

Genetic data suggest that Kin1 and Kin2 act downstream of Rho3, Cdc42, Sec4, and components of the Exocyst complex but upstream of the t-SNARE Sec9 and the Sec9-binding protein Sro7. Therefore, we hypothesized that Kin1 and Kin2 interact and function together with proteins important for the final stages of exocytosis, such as the SNAREs. To test this, we used the candidate approach to search for Kin1- and Kin2-interacting partners. First, we observed that antibodies against both Kin1 and Kin2 bring down the t-SNARE Sec9 when both genes are expressed at high copy (Figure 6A). Sec9 immunoprecipitation with Kin1 and Kin2 antibodies was detected with the endogenous levels of Kin1 and Kin2 as well (our unpublished data). To confirm that Kin1 exists in a protein complex with Sec9 by a different method, we used a chemical cross-linking procedure. Cells from strains overexpressing both *KIN1* and *SEC9* were labeled with [35 S]methionine for 1 h and then lysed. Lysed cells were treated with the chemical cross-linker DSP and subjected to two rounds of immunoprecipitation. In the first round, samples were divided into two pools and incubated with affinity-purified antibodies either against Kin1 or against Sec9, and immune complexes formed were pulled down via protein A-Sepharose. In the second round, each of the two pools was subjected to a denaturing immunoprecipitation with either anti-Sec9 or anti-Kin1 antibodies. Our results show that in the presence of the cross-linker Kin1

coimmunoprecipitates Sec9, and in its turn, Sec9 pulls down Kin1 (Figure 6B).

To identify other potential Kin1- and Kin2-interacting partners, we performed a series of native immunoprecipitation experiments testing for the association of Kin1 and Kin2 with proteins acting in the secretory pathway. Namely, we examined whether antibodies against Kin2 can pull down two other exocytic SNAREs, Sso and Snc, the Sec9-interacting protein Sro7, and the Rab GTPase Sec4. Kin2 was immunoprecipitated from the cell lysates carrying multicopy *KIN2*, and the sample was analyzed by Western blotting with α -Kin2, α -Sso2, α -Snc1, α -Sro7, and α -Sec4 antibodies, respectively. This experiment revealed that the α -Kin2 antibody brings down significant amounts of Sro7, a homologue of a tumor suppressor protein *lethal giant larvae* (Lgl), but not other proteins tested (Figure 6C). As expected, Sro7 also coimmunoprecipitates with anti-Kin1 antibodies (our unpublished data). Therefore, Kin1 and Kin2 associate with t-SNARE Sec9 and the Sec9-binding protein Sro7.

To determine whether association of Kin1 and Kin2 with Sec9 and Sro7 is a result of a direct binding between these proteins, we used a yeast two-hybrid analysis. Kin1 and Kin2 in both GAL4 binding and GAL4 activation domain fusions did not show interaction with either Sec9 or Sro7 in GAL4 activation and GAL4 binding fusions, respectively (our unpublished data). This indicates that the interaction of Kin1 and Kin2 with Sec9 and Sro7 is not direct but occurs via other intermediaries in the complex.

The physical association of Kin1 and Kin2 with the SNARE machinery supports the hypothesis that these Par-1 counterparts play a role in exocytosis at a stage between vesicle docking site recognition and fusion with the plasma membrane.

Kin1 and Kin2 Induce Phosphorylation of Sec9 In Vivo and Its Release from the Plasma Membrane to the Cytosol

Next, we focused on finding a downstream target of Kin1 and Kin2 function in the exocytic pathway. We observed that the interaction partner of Kin1 and Kin2, the t-SNARE Sec9, undergoes a size shift upon transient overexpression of the catalytically active Kin2 kinase (Figure 7A). Overexpres-

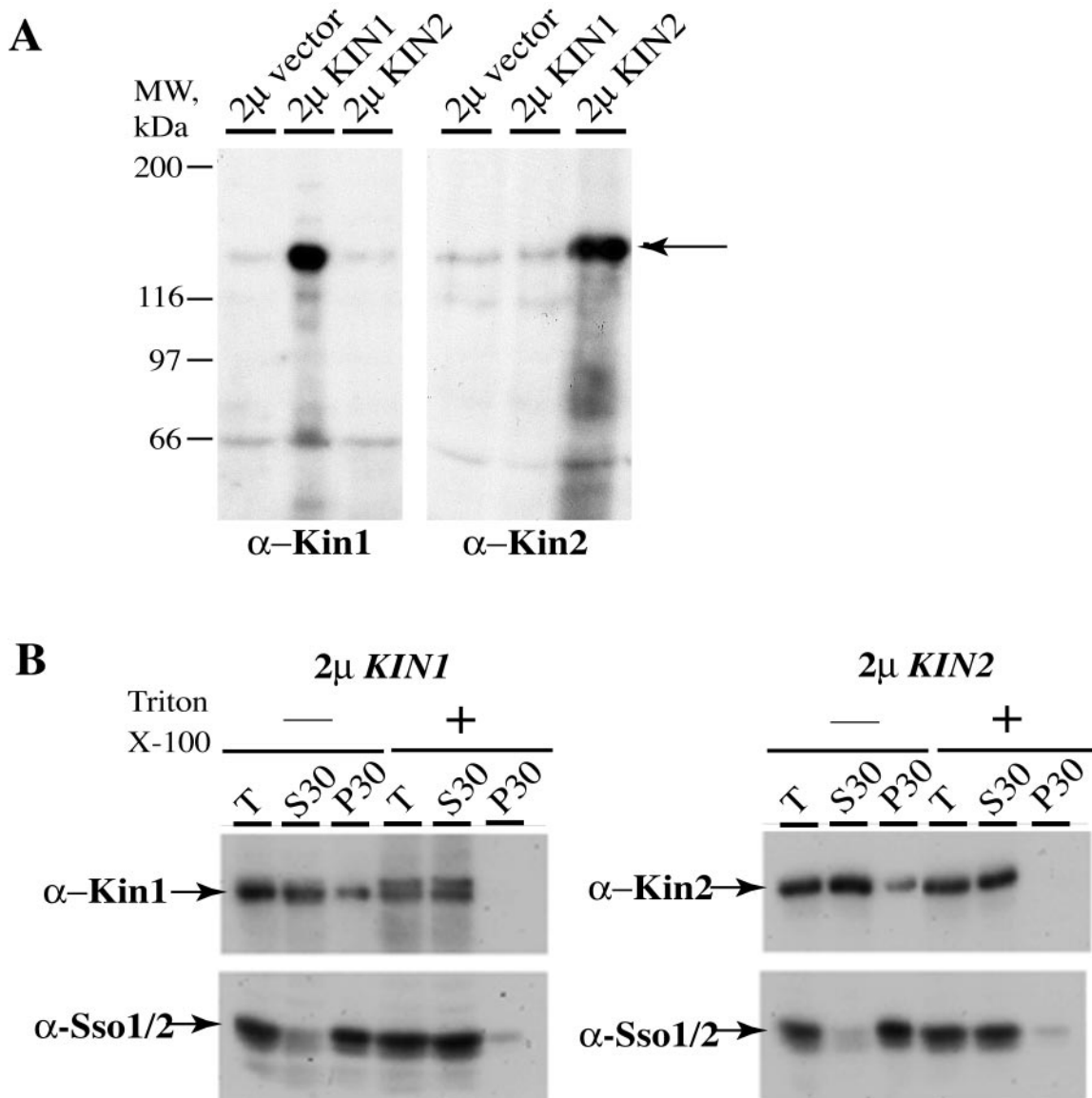


Figure 5. Kin1 and Kin2 proteins are found in both cytosolic and membrane-bound pools. (A) Affinity-purified antibodies against the C-terminal domains of Kin1 and Kin2 recognize proteins in a specific manner, running at ~ 145 kDa on SDS-PAGE. Wild-type cells and cells containing either *KIN1* or *KIN2* on high copy were subjected to 7% SDS-PAGE and Western blot by using affinity-purified antibodies against Kin1 and Kin2. (B) Kin1 and Kin2 are found in both the cytosolic and membrane-bound pools. Lysates from cells containing either vector alone, *KIN1*, or *KIN2* on high copy were treated with or without Triton X-100 and centrifuged at $30,000 \times g$ for 15 min. Supernatant and pellet fractions were analyzed (T, total; S30, supernatant; P30, pellet) by SDS-PAGE (pellet fractions were resuspended in the volume equal to that of S30 fraction) and blotted with anti-Kin1 and anti-Kin2 antibodies. Approximately 70% of both Kin1 and Kin2 is seen in the cytosolic fraction and $\sim 30\%$ is in a Triton-sensitive membrane fraction. Samples also were immunoblotted with anti-Sso1/2 polyclonal antibody as an internal control of the fractionation procedure (consistent with previous reports $\sim 80\%$ of Sso1/2 was detected in the pellet fraction).

sion of Kin1 gave a similar shift in Sec9 mobility but induction of the kinase-dead mutants of Kin1 and Kin2 failed to induce any detectable shift in Sec9 (our unpublished data). To test whether this shift is indeed the result of phosphorylation, we analyzed the effect of phosphatase treatment on the mobility of immunoprecipitated Sec9 protein after Kin2 induction. Cells carrying either vector alone or CEN/GAL *KIN2* were incubated in galactose-containing medium for 4 h to induce Kin2 expression, and lysates obtained from these cells were subjected to immunoprecipitation with anti-Sec9 antibodies. Sec9-containing immune complexes were subsequently treated with two different phosphatases:

λ -phosphatase or CIP. Phosphatase treatment, but not mock control treatment, abolished the Kin2-dependent size shift of Sec9, demonstrating that the change in Sec9 mobility in response to Kin2 induction is indeed due to phosphorylation (Figure 7A).

We next examined whether Sec9 is phosphorylated directly by Kin1/Kin2 *in vitro*. We made use of recombinant Sec9 protein as a substrate in an *in vitro* kinase reaction and looked for $[\gamma\text{-}^{32}\text{P}]\text{ATP}$ incorporation in the presence of immunoprecipitated Kin1/Kin2 proteins bound to protein A-Sepharose beads. The data shown represent phosphorylation reactions in the presence of Kin2; however, we found

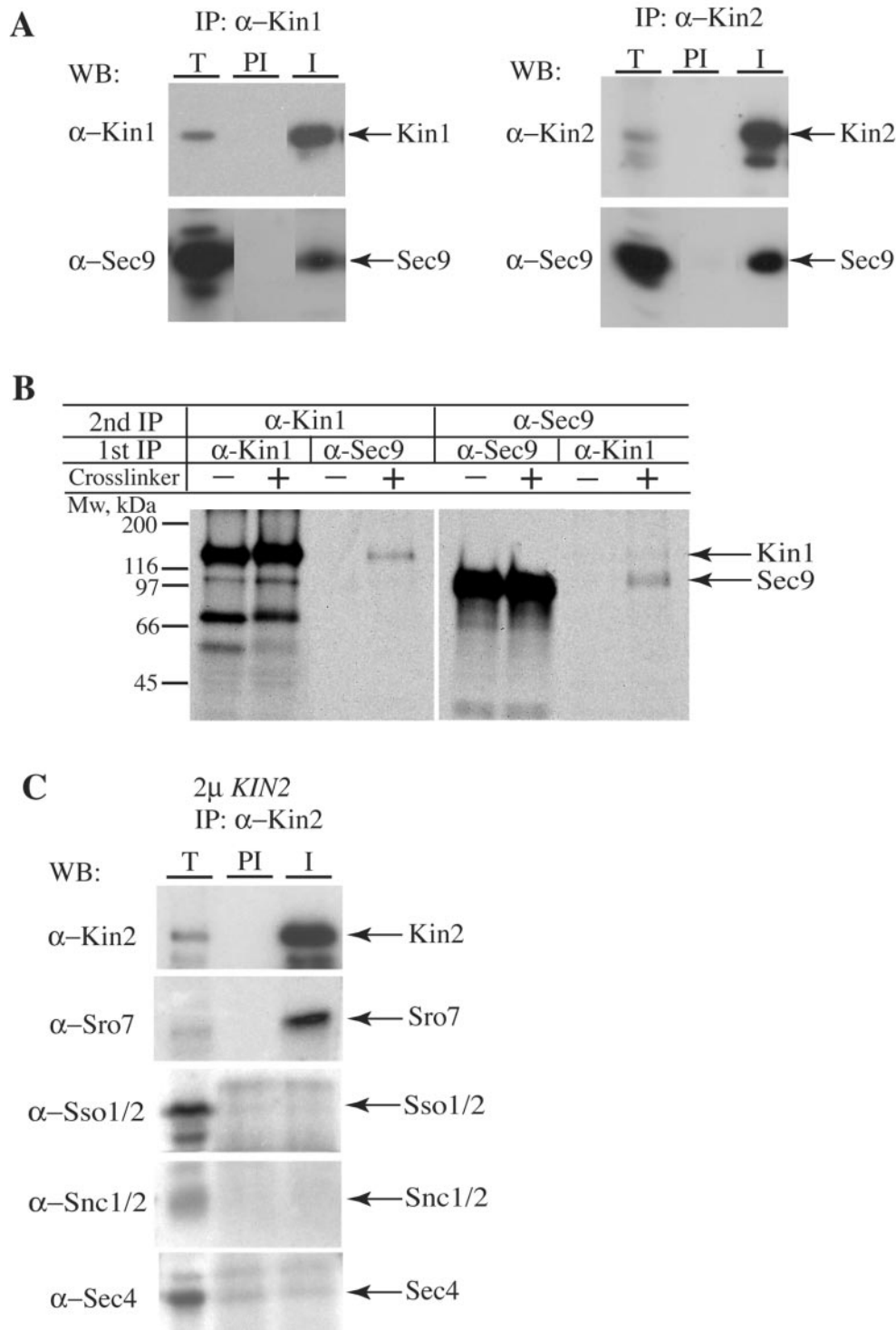


Figure 6. Kin1 and Kin2 physically associate with the t-SNARE Sec9 and the Sec9-binding protein Sro7. (A) Antibodies against Kin1 and Kin2 coimmunoprecipitate Sec9. Cell lysates carrying either high copy *KIN1* and *SEC9* or high copy *KIN2* and *SEC9* were subjected to native immunoprecipitation with preimmune serum (PI) and either anti-Kin1 or anti-Kin2 antibodies (I), respectively, as described in *Materials and Methods*. Samples were separated on 8% SDS-PAGE and immunoblotted with anti-Sec9 and either anti-Kin1 or anti-Kin2 antibodies, respectively. "T" stands for total protein in the lysate before IP, loaded at 1:20 to the amount of lysate used to immunoprecipitate Kin1 and Kin2 in PI and I lanes. (B) Cross-linking experiment confirms association between Kin1 and Sec9. Cells expressing *SEC9* and *KIN1* on a multicopy plasmid were ^{35}S -labeled for 1 h and lysed osmotically in PBS. Lysates were subjected to cross-linking, followed by two rounds of immunoprecipitations, initially with α -Kin1 and α -Sec9 antibodies, followed by a denaturing IP with α -Kin1 and α -Sec9 antibodies. Samples were run on 7% SDS-PAGE, and the ^{35}S -labeled protein was detected by autoradiography. (C) Kin2 coassociates with Sro7, but not with Snc1, Sso2, or Sec4. Lysates from cells transformed with high copy *KIN2* were subjected to native immunoprecipitation with preimmune serum (PI) and α -Kin2 antibody (I) as described in *Materials and Methods*, followed by SDS-PAGE and immunoblot with α -Kin2, α -Sro7, α -Snc1, α -Sso2, and α -Sec4 antibodies.

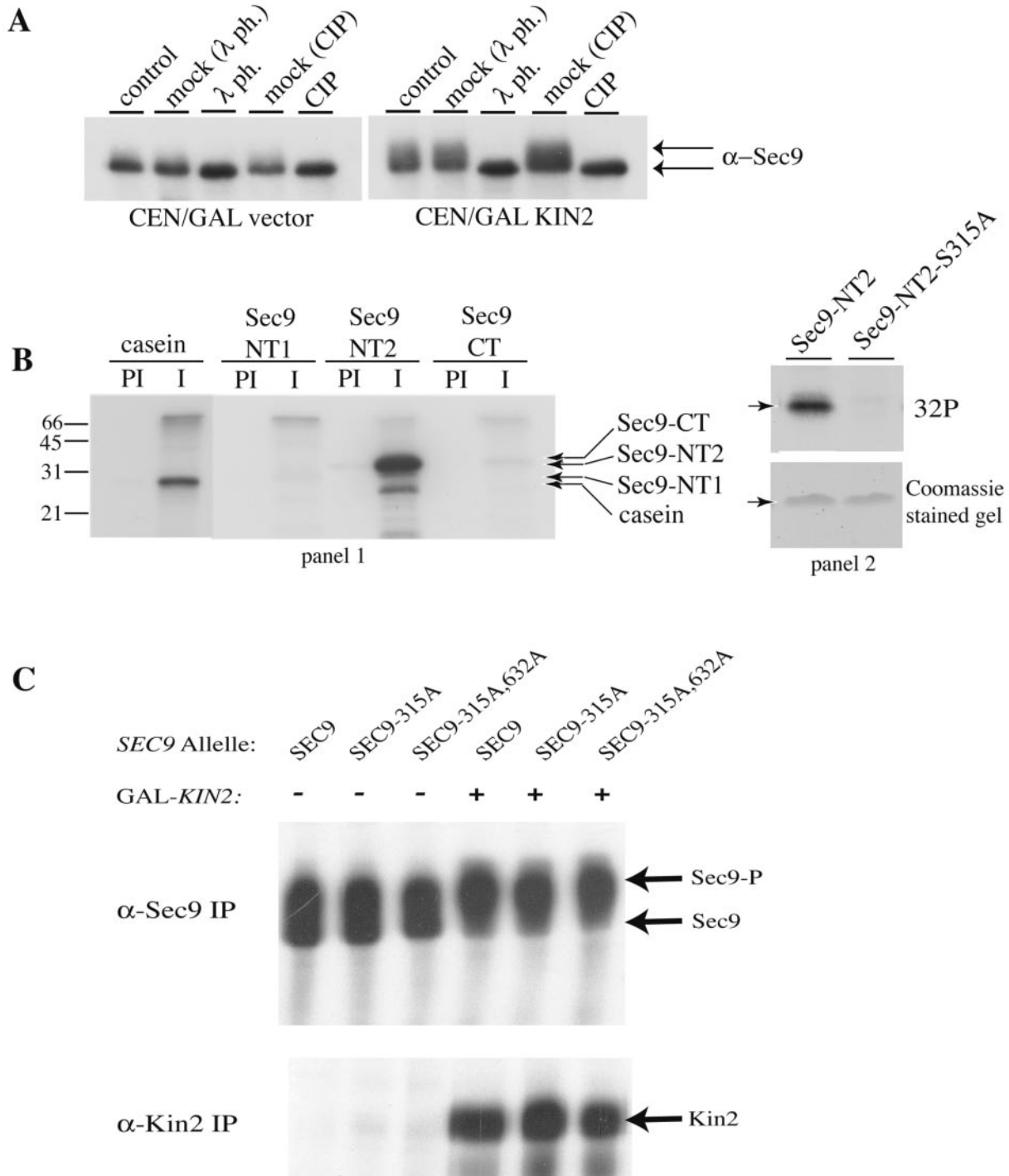


Figure 7. The t-SNARE Sec9 is phosphorylated as an effect of Kin1 or Kin2 induction. (A) Sec9 undergoes a phosphorylation-dependent size shift in response to Kin2 induction. Lysates from galactose-induced yeast cells containing high copy Sec9 and either a *CEN/GAL* vector or *CEN/GAL-KIN2* were immunoprecipitated with anti-Sec9 antibody. Immune complexes were treated with λ -phosphatase and CIP for 30 min at 30 and 37°C, respectively. Untreated and mock-treated samples, incubated under identical conditions, were used as a control. Samples were subjected to 8% SDS-PAGE and immunoblotted with α -Sec9 antibody. (B) N terminus of Sec9 is a substrate of Kin2 in vitro. Cells expressing Kin2 were subjected to immunoprecipitation with either α -Kin2 antibody (I) or preimmune serum (PI) as a negative control. Immobilized Kin2 on protein A-Sepharose beads was used for in vitro kinase assays. Equal molar amounts (1.5 μ M) of soluble recombinant Sec9-NT1 (amino acids 1–168), Sec9-NT2 (amino acids 166–401), and Sec9-CT (amino acids 402–651) were added to the reaction and incubated with [³²P]ATP for 30 min at 30°C. Samples were analyzed by SDS-PAGE and autoradiography (1). In 2, wild-type Sec9-NT2 and Sec9-NT2-S315A mutant were tested in an in vitro kinase reaction as described above. Concentrations of recombinant proteins used in the kinase reaction were measured by a Bradford protein assay, normalized to equal concentrations, and verified by Coomassie staining. (C) Sec9 is not a direct target of Kin2 in vivo. Lysates from cells containing *CEN/GAL* vector or *CEN/GAL* Kin2 containing multicopy wild-type Sec9 or mutant Sec9-S315A were induced with galactose for 4 h. Cells were then spheroplasted and lysed, and the lysates were boiled and separated by SDS-PAGE and immunoblotted with anti-Sec9. Arrows indicate Sec9 mobility shift.

virtually identical results for immunoprecipitated Kin1 in these assays. The recombinant Sec9 protein was initially divided into three domains, Sec9-NT1 (amino acids 1–168), Sec9-NT2 (amino acids 166–401), and Sec9-CT (corresponding to the SNAP25 domain amino acids 401–651), each of which were fused to GST, expressed in bacteria, and purified as described previously (Rossi *et al.*, 1997). This analysis demonstrated that the Sec9-NT2 protein turned out to be an excellent substrate for Kin2 (Figure 7B, 1), with phosphoacceptor activity significantly greater than that of casein, which was previously identified as a test substrate of Kin1 and Kin2 *in vitro* (Lamb *et al.*, 1991; Donovan *et al.*, 1994). We subsequently mapped the site of Sec9 phosphorylation by Kin2 to serine 315 by sequential deletion and mutagenesis of serine or threonine residues to alanine. In particular, we found that the substitution of serine 315 to alanine abolished the ability of Kin2 to phosphorylate Sec9-NT2 *in vitro* (Figure 7B, 2). We used the same strategy to map a significantly weaker *in vitro* phosphoacceptor site in the SNAP-25 domain of Sec9 to serine 632 (our unpublished data). We next determined the effect of the mutation of these sites on the Kin2-induced phosphorylation of Sec9 *in vivo*. Surprisingly, we found that the Sec9-S315A as well as Sec9-S315A, S632A proteins were identical to wild-type Sec9 in the Kin2 induced phosphorylation as judged by a mobility shift (Figure 7C). Therefore, the major phosphoacceptor sites on Sec9 phosphorylated by Kin2 *in vitro* are not responsible for Kin2-induced phosphorylation of Sec9 *in vivo*. This result indicates that *in vivo* Kin1/Kin2 are unlikely to directly phosphorylate Sec9, but rather this phosphorylation occurs as a downstream effect of Kin1/Kin2 induction, presumably by direct or indirect activation of a kinase, which in turn phosphorylates Sec9 at a site or sites other than serine 315.

To assess the specificity of the catalytic activity of Kin1 and Kin2, we examined whether other components of the late exocytic machinery are phosphorylated by these kinases. *In vivo* experiments were performed on cells carrying either vector alone or *CEN/GAL KIN2*, radioactively labeled with [³²P]orthophosphate during a 4-h induction of Kin2 in galactose-containing medium. Lysates from these cells were immunoprecipitated with antibodies against Sec9, Sso1/2, Sro7, and a number of components of the Exocyst complex and a subset of small GTPases involved in secretion. An identical set of strains was simultaneously labeled with [³⁵S]methionine to control for the presence of the proteins in the lysates examined. Proteins were separated on SDS-PAGE, and their phosphorylation state was determined by autoradiography. Out of all proteins tested, only Sec9 displayed an increased level of [³²P]orthophosphate incorporation in cells overexpressing Kin2 (Figure 8). Thus, Kin2 specifically induces the phosphorylation of Sec9. These data allow us to hypothesize that Kin1 and Kin2 act in the secretory pathway by regulating the phosphorylation of the t-SNARE Sec9.

To address the functional significance of the Sec9 phosphorylation induced by Kin1 and Kin2, we tested whether expression of these kinases affects the subcellular localization of Sec9. We analyzed the distribution of Sec9 into pellet and supernatant fractions after centrifugation at 30,000 × *g* in galactose-induced and uninduced cells carrying *CEN/GAL KIN1*. In uninduced cells (as well as in cells carrying empty *CEN/GAL* vector; our unpublished data) ~50–60% of Sec9 is cytosolic and partitions into the supernatant fraction, whereas the rest is membrane bound (the Triton-sensitive pellet fraction) (Figure 9). Interestingly, in cells expressing *CEN/GAL KIN1* the proportion of the cytosolic Sec9 is increased relative to the membrane-bound Sec9 (Figure 9).

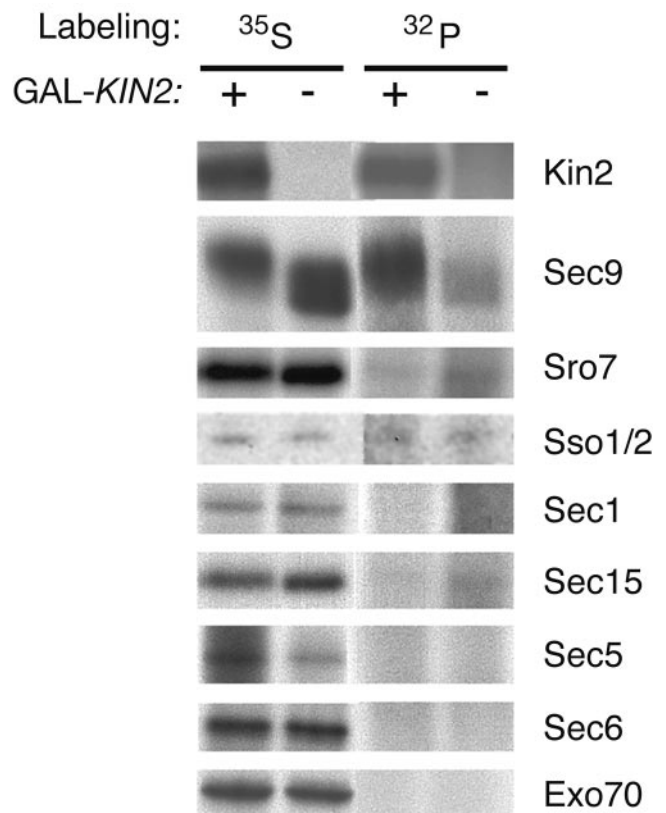
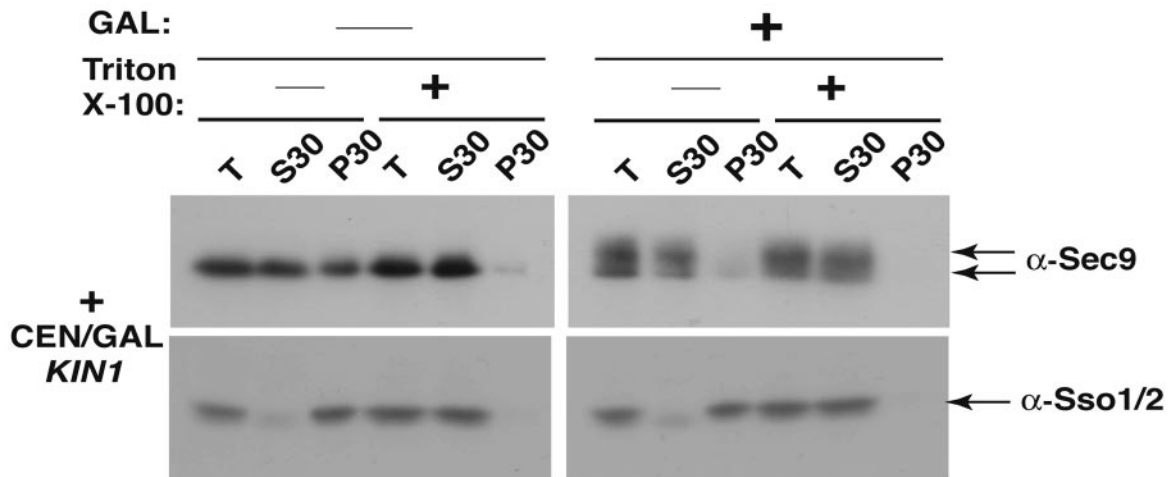
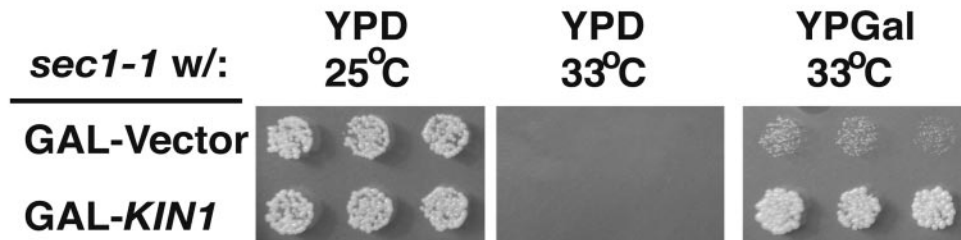


Figure 8. Sec9 is the only component of the exocytic apparatus tested that is phosphorylated upon Kin2 induction. Cells containing empty vector, or *GAL-KIN2* were induced with galactose for 2 h before labeling with either [³⁵S]methionine or [³²P]orthophosphate. Denatured cell lysates were prepared and immunoprecipitated with antibodies to the components of the late secretory machinery. Phosphate-incorporation was detected by SDS-PAGE and autoradiography. Quantitation demonstrated that when cells were induced with *GAL-KIN2*, the amount of ³²P label incorporated into Sec9 increased threefold. The small increase in ³²P labeling in the cells lacking *GAL-KIN2* was due to slight increase in overall ³²P labeling in this sample.

Averaging three independent experiments, induction of Kin1 expression resulted in reproducible elevation of the cytosolic Sec9 levels to ~70–75% of the total Sec9 pool. As expected, Kin1 does not alter distribution of Sso1/2 under identical conditions (Figure 9). Furthermore, Sec9 undergoes a Kin1-mediated mobility shift exclusively in the cytosolic but not the membrane fraction. As expected, induction of *KIN2* had the same effect on Sec9 distribution (our unpublished data). Thus, overexpression of Kin1 or Kin2 results in release of a fraction of Sec9 from the plasma membrane into the cytosol.

To determine the effect of *GAL*-induced Kin1 overexpression on overall growth and secretory function, we examined the ability of *sec1-1* cells transformed with a *GAL-KIN1* construct to grow and secrete the periplasmic protein *BglIII*. As shown in Figure 9B, we find that galactose-induced expression of Kin1 protein results in dramatic suppression of the growth defect at the nonpermissive temperature of 33°C. Suppression by *GAL-KIN1* is lost when the cells are grown on noninducing YPD media. We examined the ability of galactose induced *sec1-1* transformants to secrete *BglIII* after a shift to restrictive temperature. As shown in Figure 9C, we

A.**B.****C.**

<u>Strain</u>	<u>Genotype</u>	<u>% Bgl2 Accum.</u>
BY1	wt	16% (+/- 3.5%)
BY1552	<i>sec1-1</i> , GAL-Vector	38% (+/- 5%)
BY1553	<i>sec1-1</i> , GAL- <i>KIN1</i>	19% (+/- 2.5%)

Figure 9. Kin1 overexpression reduces the membrane association of Sec9 while increasing secretory function. (A) Fractionation of Sec9 in *GAL-KIN1* induced cells. Lysates from galactose-induced and uninduced cells containing *CEN/GAL KIN1* and high copy *SEC9* were treated with or without Triton X-100 and centrifuged at $30,000 \times g$ for 15 min. Supernatant and pellet fractions were subjected to SDS-PAGE and blotted with anti-Sec9 antibodies (T, total; S30, $30k \times g$ supernatant; P30, $30k \times g$ pellet). The proportion of Sec9 in the cytosolic and Triton-sensitive membrane fraction was quantified as an average of three independent experiments. Samples also were immunoblotted with anti-Sso1/2 polyclonal antibody as an internal control. (B) Suppression of the *sec1-1* growth defect by *GAL-KIN1*. *sec1-1* mutants were transformed with empty vector or *GAL-KIN1* and replicated for growth at permissive (25°C) and restrictive (33°C) temperatures on media that induces (YP-Gal) or represses (YPD) overexpression of the Kin1 protein. (C) Suppression of the *sec1-1* secretion defect by *GAL-KIN1*. *sec1-1* mutant strains containing empty vector or *GAL-KIN2* were induced for 2 h in galactose, shifted to 33°C for 2 h, and then processed for BglIII secretion (defects in secretion are seen as an increase in the fraction of BglIII found internally).

find that control *sec1-1* cells containing an empty *GAL* vector show an accumulation of internal BglIII. In contrast cells containing *GAL-KIN1* show a dramatic suppression of the secretory defect to levels of internal BglIII found in wild-type yeast cells. Therefore, the same conditions of Kin1 overexpression that result in a reduction of Sec9 levels on the membrane also yield an overall “gain of function” in the secretory pathway.

Based on these data, we suggest that the positive effect of Kin1 and Kin2 on the secretory pathway may be mediated through regulation of the plasma membrane t-SNARE Sec9. Consistent with this assumption, overexpression of *SEC9* suppresses growth defects of a number of late *sec* mutants that also are suppressed by introduction of multicopy *KIN1* and *KIN2*. High copy *SEC9* is known to restore the viability of *rho3Δ*, *sec4-P48*, *sec1-1*, *sec3-2*, *sec8-9*, *sec9-4*, and *sec15-1*

Table 4. Comparison of suppression properties of high copy *KIN1*, *KIN2* with those of high copy *SEC9*

Mutant	2 μ <i>KIN1</i>	2 μ <i>KIN2</i>	2 μ <i>SEC9</i>
<i>rho3-V51^{cs-}</i>	+++	+++	+++
<i>sec1-1^{ts-}</i>	+	+	++
<i>sec2-41^{ts-}</i>	++	++	—
<i>sec3-2^{ts-}</i>	+/-	+/-	++
<i>sec4-P48^{cs-}</i>	+++	+++	+++
<i>sec5-24^{ts-}</i>	—	—	—
<i>sec6-4^{ts-}</i>	—	—	—
<i>sec8-9^{ts-}</i>	—	—	++
<i>sec9-4^{ts-}</i>	—	—	+++
<i>sec10-2^{ts-}</i>	++	++	++
<i>sec15-1^{ts-}</i>	+++	+++	+++
<i>sro7Δ, sro77Δ</i>	—	—	—

Secretory mutants were transformed with either vector (pRS426), *KIN1*, *KIN2*, or *SEC9* on high copy. Growth of transformants at permissive (25°C) and restrictive temperatures was tested. The following restrictive temperatures were applied: 14°C for *rho3-V51*, 33°C for *sec1-1*, 33°C for *sec2-41*, 35°C for *sec3-2*, 14°C for *sec4-P48*, 33°C for *sec5-24*, 35°C for *sec6-4*, 37°C for *sec8-9*, 34°C for *sec9-4*, 35°C for *sec10-2*, 35°C for *sec15-1*, and 19°C for *sro7 Δ , sro77 Δ* . Scoring reflects the mutant colony growth at their respective restrictive temperatures relative to the wild-type yeast (+++) and empty vector control (—). Suppression of the *sec* mutants is indicated as follows: +++, very strong; ++, strong; +, moderate; +/-, weak.

(Lehman *et al.*, 1999). When we compared the relative suppression capabilities of high copy *KIN1*, *KIN2*, and *SEC9*, we found that *KIN1* and *KIN2* largely mimic the *SEC9* suppression profile and exert an effect either equal or less potent in comparison with that of *SEC9* (Table 4). The only mutant that *KIN1* and *KIN2*, but not *SEC9*, are capable of suppressing is *sec2-41*, the significance of which remains to be addressed. Together, our results are consistent with Kin1 and Kin2 acting in the secretory pathway by positively regulating Sec9 function.

DISCUSSION

Novel Role for Par-1: Regulation of Exocytosis

Par-1 is a key regulator of polarity-axis formation in a number of organisms. This includes the anterior-posterior axis of the *C. elegans* zygote and the *Drosophila* oocyte and the apico-basal axis of polarized epithelia in *Drosophila* and mammalian cells. Par-1 has been proposed to regulate cell fate determination and polarized cell morphology by positioning polarity markers, modulating activity of signaling pathways such as Wnt (canonical) and phencyclidine (planar cell polarity) and reorganizing the microtubule cytoskeleton (Kemphues *et al.*, 1988; Drewes *et al.*, 1997; Tenenhaus *et al.*, 1998; Shulman *et al.*, 2000; Cox *et al.*, 2001; Huynh *et al.*, 2001; Sun *et al.*, 2001; Vaccari and Ephrussi, 2002; Benton and Johnston, 2003; Doerflinger *et al.*, 2003; Cohen *et al.*, 2004).

This is the first report linking Par-1 to regulation of exocytosis. Here, we show that the yeast Par-1 counterparts Kin1 and Kin2 exhibit multiple genetic and physical interactions with components of the exocytic machinery and thus function in the post-Golgi secretory pathway in *S. cerevisiae*. We demonstrate that both *KIN1* and *KIN2* suppress the growth abnormality of *rho3 Δ , rho3-V51, sec1, sec2, sec3, sec4, sec10*, and *sec15*, mutants of genes important for polarized vesicle transport and docking. However, we observed that

neither *KIN1* nor *KIN2* suppress *sec9-4* and *sro7 Δ , sro77 Δ* , which are mutants of proteins involved in SNARE complex assembly and fusion. Thus, our genetic data position Kin1 and Kin2 function between the vesicle docking and fusion stages of exocytosis and identify these kinases as downstream effectors of the small GTPases: Rho3, Cdc42, Sec4, and several components of the vesicle tethering machinery. Moreover, these structurally homologous proteins display functional redundancy as well, because they show an identical pattern of suppression of the late secretory mutants. Consistent with genetic evidence, the analysis of physical associations of Kin1 and Kin2 show that these proteins exist in a complex with proteins necessary for fusion of exocytic vesicles with the plasma membrane. We demonstrate that Kin1 and Kin2 coimmunoprecipitate with the t-SNARE Sec9, and the homologue of the *Drosophila* tumor suppressor *lethal giant larvae*, Sro7, which has been previously reported to bind to Sec9 (Lehman *et al.*, 1999). Based on physical and genetic data, we propose that Kin1 and Kin2 transmit a signal from the upstream-acting GTPases and the docking complex to the SNARE proteins to ensure correct vesicle fusion.

How conserved is the role of Par-1 in exocytosis? A high degree of functional conservation was observed for proteins constituting the Golgi-to-cell surface vesicle delivery machinery, including the Exocyst complex and the SNARE proteins (Kee *et al.*, 1997; Rossi *et al.*, 1997). Therefore, potentially, a link between Par-1 and the polarized exocytic machinery might represent a universal feature. Remarkably, a collaboration with Dr. Anne Muesch (Cornell Medical College, Ithaca, NY) revealed that mammalian Par-1 (EMK1) exists in a protein complex with the basolateral t-SNARE Syntaxin 4 and the Exocyst components in Madin-Darby canine kidney (MDCK) cells (our unpublished data, personal communication), suggesting that Par-1 is involved in the regulation of exocytosis in polarized mammalian cells as well. Nevertheless, there are some differences between the two systems. In MDCK cells, EMK1 interacts with the t-SNARE Syntaxin 4 but not with the mammalian equivalent of Sec9, SNAP25. On the other hand, our group did not detect any association between Kin1/Kin2 and Sso1/2, the yeast counterparts of the mammalian syntaxins. Thus, although Par-1 function in exocytosis is likely to be conserved, the precise molecular mechanism of signal transduction by Par-1 might differ from species to species.

Mechanism of Kin1 and Kin2 Function

Analysis of a kinase-dead mutant of Kin1 and Kin2 in yeast showed that the catalytic activity of these kinases is essential for suppression of *sec* mutants and thus for function in exocytosis. Therefore, we focused on finding a target and downstream effector of Kin1 and Kin2 in the secretory pathway. We assessed the ability of these kinases to phosphorylate a number of components of the late exocytic machinery, including the post-Golgi SNAREs. We found that the t-SNARE Sec9 is the only protein out of those tested that is phosphorylated *in vivo* upon overexpression of Kin1 and Kin2. Although we cannot exclude the possibility that another, as yet untested, component of the exocytic machinery is the target of Kin1/2 function in this pathway, the genetic and biochemical evidence provided here strongly suggests that Sec9 is the ultimate target of Kin1/2 action on exocytosis. Despite the fact that Sec9 can serve as a direct substrate of Kin1 and Kin2 *in vitro*, analysis of a phospho-mutant of Sec9 revealed that *in vivo* Kin1/Kin2-mediated phosphorylation of Sec9 is likely to be indirect. It is presently unclear

which protein kinase transmits the signal from Kin1/Kin2 to Sec9.

How is the t-SNARE Sec9 regulated by yeast Par-1 orthologues? Recent studies demonstrated that SNARE protein stability, localization, and assembly into functional complexes are amenable to regulation by phosphorylation and dephosphorylation as is the final process of membrane fusion itself (Foster *et al.*, 1998; Cabaniols *et al.*, 1999; Peters *et al.*, 1999; Risinger and Bennett, 1999; Chung *et al.*, 2000; Kataoka *et al.*, 2000; Lin and Scheller, 2000; Verona *et al.*, 2000; Marash and Gerst, 2001; Pombo *et al.*, 2001; Nagy *et al.*, 2002, 2004; Polgar *et al.*, 2003; Tian *et al.*, 2003). Here, we show that Kin1 and Kin2 alter the intracellular distribution of Sec9. At steady state, Sec9 is distributed approximately equally between the cytosol and the membrane. We observed that expression of Kin1 and Kin2 results in depletion of the membrane pool of Sec9 and induces phosphorylation of cytosolic Sec9. Thus, yeast Par-1 orthologues either release membrane-bound Sec9 or prevent its attachment to the membrane by yet unknown mechanism involving phosphorylation of the t-SNARE. Our data suggest that Kin1 and Kin2 transmit a signal to the secretory pathway by increasing the level and, possibly, activity of Sec9 in the cytosol. Consistent with this, overexpression of *KIN1* and *KIN2* produced the same effect as overexpression of *SEC9* with respect to restoration of the growth of a number of *sec* mutants. The only mutant that we found to be rescued by *KIN1* and *KIN2*, but not by *SEC9* overexpression, is *sec2*, encoding an exchange factor for Sec4. It can be either due to Kin1/Kin2 having an additional function independent of regulation of Sec9, or alternatively, Sec9 might require Kin1/Kin2-induced phosphorylation to gain suppression of *sec2*.

The increase in the proportion of Sec9 in the cytosol induced by Kin1 and Kin2 suggests a mechanism by which their action promotes exocytosis. Previous work has suggested that Sec9 represents the limiting component in the formation of plasma membrane SNARE complexes and is present in wild-type cells in molar amounts that are 5- to 10-fold lower than the other two SNAREs it forms complexes with: Sso1/2 and Snc1/2 (Brennwald *et al.*, 1994). Therefore increasing amounts of Sec9 available for formation of SNARE complexes either by increasing overall Sec9 protein levels (i.e., increasing *SEC9* dosage) or increasing the proportion of free Sec9 available to form SNARE complexes would be expected to have strong positive effect on exocytic activity. However, it is known that SNARE complex assembly occurs on the plasma membrane. How does the Kin1/2-mediated release of Sec9 from the membrane into the cytosol promote exocytosis?

It is likely that Kin1 and Kin2 phosphorylate and release from the membrane free, unassembled Sec9 for two reasons. First, we have not detected the interaction between Kin1/Kin2 and two other exocytic SNAREs: the t-SNARE Sso and the v-SNARE Snc. Second, we have not detected a dramatic difference in the amount of Sec9 present in SNARE complexes as a consequence of Kin1 or Kin2 activity (our unpublished observation), and thus this pathway does not affect steady-state amounts of SNARE complexes present. Nevertheless, it cannot be ruled out that Kin1 and Kin2 phosphorylate a fraction of Sec9 in "old", inactive SNARE complexes and initiate its release, priming Sec9 for a new round of vesicle fusion.

Importantly, although it may seem contradictory that elevation of unassembled SNARE levels in the cytosol at the expense of the membrane-bound pool promotes vesicle fusion, we hypothesize that Sec9 is recruited from the cytosolic rather than the membrane pool into new SNARE complexes.

Under this assumption, the more efficient release of Sec9 from the membrane induced by Kin1 and Kin2 phosphorylation replenishes the pool of assembly-competent Sec9 near sites of recruitment. Consequently, increased cycling of Sec9 would promote complex assembly and vesicle fusion. Thus, we think that Kin1 and Kin2 promote secretion by increasing the pool of Sec9 available for incorporation into new, active SNARE complexes.

It is also possible that Kin1 and Kin2 help to spatially direct SNARE complex formation by locally priming Sec9 for assembly. In *S. cerevisiae* fusion of vesicles is restricted to the tip of the bud. Nevertheless, the t-SNARE Sec9 is not polarized, in fact, it localizes ubiquitously in the cytoplasm and homogeneously over the entire perimeter of the plasma membrane (Brennwald *et al.*, 1994). Distribution of the other t-SNARE, Sso, is also nonpolar (Brennwald *et al.*, 1994). Therefore, other molecules are required to restrict formation of fusion-competent SNARE complexes to the bud tip. Exogenous Kin1 and Kin2 localize ubiquitously in the cell (our unpublished observation). However, based on our genetic data, these kinases act downstream of molecules directing polarized vesicle transport and docking, such as Rho3, Cdc42, Sec4, and the Exocyst complex. Thus, Kin1 and Kin2 are likely to be activated and regulate Sec9 in a polarized manner, possibly by phosphorylating and releasing Sec9 from the membrane locally, near the sites of fusion.

Structural Insights: the Conserved 42-Amino Acid Tail Function in Autoinhibition

The C-terminal 42 amino acid tail sequence (termed "KA1" domain) is highly conserved throughout Par-1 orthologues from yeast to mammalian cells. Nevertheless, the role of this conserved segment remained unknown. Our data show that deletion of these 42 amino acids results in the gain of function of the kinase in the secretory pathway. Kin2 constructs with a deletion of the tail display stronger suppression of the growth defect of *sec* mutants relative to the wild-type kinase, suggesting that the tail plays an inhibitory role. Binding of the regulatory domain of the kinase to its catalytic core is a known mechanism of kinase autoinhibition (Hu *et al.*, 1994; Tu *et al.*, 1997; Tu and Wigler, 1999; Tan *et al.*, 2001). Inhibition can happen via two scenarios: in *cis*, with one molecule circling on itself (as shown in Figure 3D), and in *trans*, mediated through head-to-tail dimer formation. In a "closed" configuration an inhibitory segment inactivates a kinase by blocking either the ATP- or the substrate-binding sites. Consistent with this mechanism of autoinhibition, we show that catalytic (N-terminal) and regulatory (C-terminal) domains of Kin2 directly interact with each other and that this interaction requires an intact 42 amino acid tail sequence. Hence, we provide functional and physical evidence for the inhibitory role of the C-terminal tail. Considering a remarkable degree of conservation of the tail sequence between Par-1 orthologues, it is likely that the autoinhibitory function of the tail is conserved as well.

CONCLUSIONS

In summary, we report three novel findings. First, we demonstrate that yeast Par-1 counterparts are associated with and seem to positively regulate the function of the exocytic apparatus. Second, we show that Kin1 and Kin2 induce phosphorylation of Sec9 and its release from the plasma membrane to the cytosol, promoting its recycling and/or availability for incorporation into newly formed SNARE complexes. Third, we find that the conserved 42-amino acid

tail of the yeast Par-1 orthologues plays a role in autoinhibition.

This suggests an interesting possibility that the role of Par-1 in cell polarity establishment in a variety of organisms might be tied to the control of Golgi-to-plasma membrane vesicle targeting. It is possible to envision that the primary function of Par-1 is to regulate polarized secretion, which in turn is necessary for proper localization of polarity determinants and microtubule capture/stabilization, processes that require Par-1 in a number of species. It remains to be seen how essential and conserved is the function of Par-1 in exocytosis.

ACKNOWLEDGMENTS

We thank Drs. Anne Muesch, Enrique Rodriguez-Boulan, and Guido Wendel for invaluable advice and critical comments on the manuscript. This work was supported by The National Institutes of Health grant GM-54712 (to P. B.) and The Tri-Institutional Training Program in Vision Research grant T32EY007138 (to M. E.).

REFERENCES

- Aalto, M. K., Ronne, H., and Keranen, S. (1993). Yeast syntaxins Sso1p and Sso2p belong to a family of related membrane proteins that function in vesicular transport. *EMBO J.* *12*, 4095–4104.
- Adamo, J. E., Moskow, J. J., Gladfelter, A. S., Viterbo, D., Lew, D. J., and Brennwald, P. J. (2001). Yeast Cdc42 functions at a late step in exocytosis, specifically during polarized growth of the emerging bud. *J. Cell Biol.* *155*, 581–592.
- Adamo, J. E., Rossi, G., and Brennwald, P. (1999). The Rho GTPase Rho3 has a direct role in exocytosis that is distinct from its role in actin polarity. *Mol. Biol. Cell* *10*, 4121–4133.
- Becker, D. M., and Guarente, L. (1991). High-efficiency transformation of yeast by electroporation. *Methods Enzymol.* *194*, 182–187.
- Benton, R., and Johnston, D. S. (2003). *Drosophila* PAR-1 and 14-3-3 inhibit Bazooka/PAR-3 to establish complementary cortical domains in polarized cells. *Cell* *115*, 691–704.
- Bohm, H., Brinkmann, V., Drab, M., Henke, A., and Kurczalia, T. V. (1997). Mammalian homologues of *C. elegans* PAR-1 are asymmetrically localized in epithelial cells and may influence their polarity. *Curr. Biol.* *7*, 603–606.
- Brennwald, P., Kearns, B., Champion, K., Keranen, S., Bankaitis, V., and Novick, P. (1994). Sec9 is a SNAP-25-like component of a yeast SNARE complex that may be the effector of Sec4 function in exocytosis. *Cell* *79*, 245–258.
- Cabaniols, J. P., Ravichandran V, and Roche, P. A. (1999). Phosphorylation of SNAP-23 by the novel kinase SNAK regulates t-SNARE complex assembly. *Mol. Biol. Cell* *10*, 4033–4041.
- Carr, C. M., Grote, E., Munson, M., Hughson, F. M., and Novick, P. J. (1999). Sec1p binds to SNARE complexes and concentrates at sites of secretion. *J. Cell Biol.* *146*, 333–344.
- Celenza, J. L., and Carlson, M. (1984). Structure and expression of the SNF1 gene of *Saccharomyces cerevisiae*. *Mol. Cell. Biol.* *4*, 54–60.
- Chung, S. H., Polgar, J., and Reed, G. L. (2000). Protein kinase C (PKC) phosphorylation of syntaxin 4 in thrombin-activated human platelets. *J. Biol. Chem.* *275*, 25286–25291.
- Cohen, D., Brennwald, P. J., Rodriguez-Boulan, E., and Musch, A. (2004). Mammalian PAR-1 determines epithelial lumen polarity by organizing the microtubule cytoskeleton. *J. Cell Biol.* *164*, 717–727.
- Cox, D. N., Lu, B., Sun, T. Q., Williams, L. T., and Jan, Y. N. (2001). *Drosophila* par-1 is required for oocyte differentiation and microtubule organization. *Curr. Biol.* *11*, 75–87.
- Doerflinger, H., Benton, R., Shulman, J. M., and St Johnston, D. (2003). The role of PAR-1 in regulating the polarised microtubule cytoskeleton in the *Drosophila* follicular epithelium. *Development* *130*, 3965–3975.
- Donovan, M., Romano, P., Tibbetts, M., and Hammond, C. I. (1994). Characterization of the KIN2 gene product in *Saccharomyces cerevisiae* and comparison between the kinase activities of p145KIN1 and p145KIN2. *Yeast* *10*, 113–124.
- Drewes, G., Ebneth, A., Preuss, U., Mandelkow, E. M., and Mandelkow, E. (1997). MARK, a novel family of protein kinases that phosphorylate microtubule-associated proteins and trigger microtubule disruption. *Cell* *89*, 297–308.
- Drewes, G., Trinczek, B., Illenberger, S., Biernat, J., Schmitt-Ulms, G., Meyer, H. E., Mandelkow, E. M., and Mandelkow, E. (1995). Microtubule-associated protein/microtubule affinity-regulating kinase (p110mark). A novel protein kinase that regulates tau-microtubule interactions and dynamic instability by phosphorylation at the Alzheimer-specific site serine 262. *J. Biol. Chem.* *270*, 7679–7688.
- Foster, L. J., Y. B., Mohtashami, M., Ross, K., Trimble, W. S., and Klip, A. (1998). Binary interactions of the SNARE proteins syntaxin-4, SNAP23, and VAMP-2 and their regulation by phosphorylation. *Biochemistry* *37*, 11089–11096.
- Guo, W., Roth, D., Walch-Solimena, C., and Novick, P. (1999). The exocyst is an effector for Sec4p, targeting secretory vesicles to sites of exocytosis. *EMBO J.* *18*, 1071–1080.
- Guthrie, C. and Fink, G. (1991). Guide to yeast genetics and molecular biology. In: *Methods in Enzymology*. San Diego, CA: Academic Press.
- Hanks, S. K., Quinn, A. M., and Hunter, T. (1988). The protein kinase family: conserved features and deduced phylogeny of the catalytic domains. *Science* *241*, 42–52.
- Hu, S. H., Parker, M. W., Lei, J. Y., Wilce, M. C., Benian, G. M., and Kemp, B. E. (1994). Insights into autoregulation from the crystal structure of twitchin kinase. *Nature* *369*, 581–584.
- Huynh, J. R., Shulman, J. M., Benton, R., and St Johnston, D. (2001). PAR-1 is required for the maintenance of oocyte fate in *Drosophila*. *Development* *128*, 1201–1209.
- Imai, J., Toh-e, A., and Matsui, Y. (1996). Genetic analysis of the *Saccharomyces cerevisiae* RHO3 gene, encoding a rho-type small GTPase, provides evidence for a role in bud formation. *Genetics* *142*, 359–369.
- Kataoka, M., K. R., Iwasaki, S., Shoji-Kasai, Y., and Takahashi, M. (2000). Nerve growth factor-induced phosphorylation of SNAP-25 in PC12 cells: a possible involvement in the regulation of SNAP-25 localization. *J. Neurochem.* *74*, 2058–2066.
- Kee, Y., Yoo, J. S., Hazuka, C. D., Peterson, K. E., Hsu, S. C., and Scheller, R. H. (1997). Subunit structure of the mammalian exocyst complex. *Proc. Natl. Acad. Sci. USA* *94*, 14438–14443.
- Kemphues, K. J., Priess, J. R., Morton, D. G., and Cheng, N. S. (1988). Identification of genes required for cytoplasmic localization in early *C. elegans* embryos. *Cell* *52*, 311–320.
- Lamb, A., Tibbetts, M., and Hammond, C. I. (1991). The product of the KIN1 locus in *Saccharomyces cerevisiae* is a serine/threonine-specific protein kinase. *Yeast* *7*, 219–228.
- Lehman, K., Rossi, G., Adamo, J. E., and Brennwald, P. (1999). Yeast homologues of tomosyn and lethal giant larvae function in exocytosis and are associated with the plasma membrane SNARE, Sec9. *J. Cell Biol.* *146*, 125–140.
- Levin, D. E., and Bishop, J. M. (1990). A putative protein kinase gene (kin1+) is important for growth polarity in *Schizosaccharomyces pombe*. *Proc. Natl. Acad. Sci. USA* *87*, 8272–8276.
- Levin, D. E., Hammond, C. I., Ralston, R. O., and Bishop, J. M. (1987). Two yeast genes that encode unusual protein kinases. *Proc. Natl. Acad. Sci. USA* *84*, 6035–6039.
- Lin, R. C., and Scheller, R. H. (2000). Mechanisms of synaptic vesicle exocytosis. *Annu. Rev. Cell Dev. Biol.* *16*, 19–49.
- Marash, M., and Gerst, J. (2001). t-SNARE dephosphorylation promotes SNARE assembly and exocytosis in yeast. *EMBO J.* *20*, 411–421.
- Nagy, G., Matti, U., Nehring, R. B., Binz, T., Rettig, J., Neher, E., and Sorensen, J. B. (2002). PKC-dependent phosphorylation of synaptosome-associated protein of 25 kDa at Ser187 potentiates vesicle recruitment. *J. Neurosci.* *22*, 9278–9286.
- Nagy, G., Reim, K., Matti, U., Brose, N., Binz, T., Rettig, J., Neher, E., and Sorensen, J. B. (2004). Regulation of releasable vesicle pool sizes by protein kinase A-dependent phosphorylation of SNAP-25. *Neuron* *41*, 417–429.
- Peters, C., Andrews, P. D., Stark, M. J., Cesaro-Tadic, S., Glatz, A., Podtelejnikov, A., Mann, M., and Mayer, A. (1999). Control of the terminal step of intracellular membrane fusion by protein phosphatase 1. *Science* *285*, 1084–1087.
- Polgar, J., Lane, W. S., Chung, S. H., Houg, A. K., and Reed, G. L. (2003). Phosphorylation of SNAP-23 in activated human platelets. *J. Biol. Chem.* *278*, 44369–44376.
- Pombo, I., Martin-Verdeaux, S., Iannascoli, B., Le Mao, J., Deriano, L., Rivera, J., and Blank, U. (2001). IgE receptor type I-dependent regulation of a Rab3D-

- associated kinase: a possible link in the calcium-dependent assembly of SNARE complexes. *J. Biol. Chem.* 276, 42893–42900.
- Protopopov, V., Govindan, B., Novick, P., and Gerst, J. E. (1993). Homologs of the synaptobrevin/VAMP family of synaptic vesicle proteins function on the late secretory pathway in *S. cerevisiae*. *Cell* 74, 855–861.
- Rice, L. M., Brennwald, P., and Brunger, A. T. (1997). Formation of a yeast SNARE complex is accompanied by significant structural changes. *FEBS Lett.* 415, 49–55.
- Risinger, C., and Bennett, M. K. (1999). Differential phosphorylation of syntaxin and synaptosome-associated protein of 25 kDa (SNAP-25) isoforms. *J. Neurochem.* 72, 614–624.
- Robinson, N. G., Guo, L., Imai, J., Toh, E. A., Matsui, Y., and Tamanoi, F. (1999). Rho3 of *Saccharomyces cerevisiae*, which regulates the actin cytoskeleton and exocytosis, is a GTPase which interacts with Myo2 and Exo70. *Mol. Cell. Biol.* 19, 3580–3587.
- Rossi, G., Salminen, A., Rice, L. M., Brunger, A. T., and Brennwald, P. (1997). Analysis of a yeast SNARE complex reveals remarkable similarity to the neuronal SNARE complex and a novel function for the C terminus of the SNAP-25 homolog, Sec9. *J. Biol. Chem.* 272, 16610–16617.
- Shulman, J. M., Benton, R., and St Johnston, D. (2000). The *Drosophila* homolog of *C. elegans* PAR-1 organizes the oocyte cytoskeleton and directs oskar mRNA localization to the posterior pole. *Cell* 101, 377–388.
- Sun, T. Q., Lu, B., Feng, J. J., Reinhard, C., Jan, Y. N., Fantl, W. J., and Williams, L. T. (2001). PAR-1 is a Dishevelled-associated kinase and a positive regulator of Wnt signalling. *Nat. Cell Biol.* 3, 628–636.
- Tan, I., Seow, K. T., Lim, L., and Leung, T. (2001). Intermolecular and intramolecular interactions regulate catalytic activity of myotonic dystrophy kinase-related Cdc42-binding kinase alpha. *Mol. Cell. Biol.* 21, 2767–2778.
- Tenenhaus, C., Schubert, C., and Seydoux, G. (1998). Genetic requirements for PIE-1 localization and inhibition of gene expression in the embryonic germ lineage of *Caenorhabditis elegans*. *Dev. Biol.* 200, 212–224.
- TerBush, D. R., and Novick, P. (1995). Sec6, Sec8, and Sec15 are components of a multisubunit complex which localizes to small bud tips in *Saccharomyces cerevisiae*. *J. Cell Biol.* 130, 299–312.
- Tian, J. H., Das, S., and Sheng, Z. H. (2003). Ca²⁺-dependent phosphorylation of syntaxin-1A by the death-associated protein (DAP) kinase regulates its interaction with Munc18. *J. Biol. Chem.* 278, 26265–26274.
- Tibbetts, M., Donovan, M., Roe, S., Stiltner, A. M., and Hammond, C. I. (1994). KIN1 and KIN2 protein kinases localize to the cytoplasmic face of the yeast plasma membrane. *Exp. Cell Res.* 213, 93–99.
- Tomancak, P., Piano, F., Riechmann, V., Gunsalus, K. C., Kempfues, K. J., and Ephrussi, A. (2000). A *Drosophila melanogaster* homologue of *Caenorhabditis elegans* par-1 acts at an early step in embryonic-axis formation. *Nat. Cell Biol.* 2, 458–460.
- Tu, H., Barr, M., Dong, D. L., and Wigler, M. (1997). Multiple regulatory domains on the Byr2 protein kinase. *Mol. Cell. Biol.* 17, 5876–5887.
- Tu, H., and Wigler, M. (1999). Genetic evidence for Pak1 autoinhibition and its release by Cdc42. *Mol. Cell. Biol.* 19, 602–611.
- Vaccari, T., and Ephrussi, A. (2002). The fusome and microtubules enrich Par-1 in the oocyte, where it effects polarization in conjunction with Par-3, BicD, Egl, and dynein. *Curr. Biol.* 12, 1524–1528.
- Verona, M., Zanotti, S., Schafer, T., Racagni, G., and Popoli, M. (2000). Changes of synaptotagmin interaction with t-SNARE proteins in vitro after calcium/calmodulin-dependent phosphorylation. *J. Neurochem.* 74, 209–221.
- Walch-Solimena, C., Collins, R. N., and Novick, P. J. (1997). Sec2p mediates nucleotide exchange on Sec4p and is involved in polarized delivery of post-Golgi vesicles. *J. Cell Biol.* 137, 1495–1509.